A Jigsaw Puzzle based Reconfiguration Technique for Enhancing Maximum Power in Partial Shaded Hybrid Photovoltaic Array

Palpandian M (palpandianm@gmail.com)
Thamirabharani Engineering College https://orcid.org/0000-0002-5219-0470
Prince Winston David
Kamaraj College of Engineering and Technology
Rajvikram Madurai Elavarasan
Texas A&M University at Galveston
Pounraj Periyasamy
Central University of Karnataka
Rishi Pugazhendhi
Sri Venkateshwara College of Engineering
GM Shafiullah
Murdoch University
Sendhil Kumar Natarajan
National Institute of Technology Puducherry

Research Article

Keywords: Partial shading condition, hybrid configuration, jigsaw puzzle pattern, global maximum power point, performance ratio

Posted Date: May 18th, 2021

DOI: https://doi.org/10.21203/rs.3.rs-513975/v1

A jigsaw puzzle based reconfiguration technique for enhancing maximum power in partial shaded hybrid photovoltaic array

Palpandian Murugesan[1*], Prince Winston David[2], Rajvikram Madurai Elavarasan [3*], Pounraj Periyasamy[4], Rishi Pugazhendhi[5], GM Shafiullah[6], Sendhil Kumar Natarajan[7]

[1] Department of Electrical and Electronics Engineering, Thamirabharani Engineering College, Tirunelveli 627358, Tamil Nadu, India; palpandianm@gmail.com.

[2] Department of Electrical and Electronics Engineering, Kamaraj College of Engineering and Technology, Virudhunagar, 626001, Tamil Nadu, India; dpwtce@gmail.com.

[3] Clean and Resilient Energy Systems Laboratory, Texas A&M University, Galveston, TX 77553, USA; rajvikram787@gmail.com.

[4] Department of Electrical Engineering, School of Engineering, Central University of Karnataka, Kadaganchi, Kalaburagi - 585367, Karnataka,India; eeepounrajssce@gmail.com.

[5] Department of Mechanical Engineering , Sri Venkateshwara College of Engineering, Chennai, India; rishi2000.p@gmail.com.

[6] Discipline of Engineering and Energy, Murdoch University, Murdoch 6150, Australia; GM.shafiullah@murdoch.edu.au.

[7] Department of Mechanical Engineering, NIT - Puducherry, Karaikal – 609609, U.T of Puducherry, India; drsendhil1980iitmuk@gmail.com

Correspondence

Palpandian Murugesan[1], Department of Electrical and Electronics Engineering, Thamirabharani Engineering College, Tirunelveli 627358, Tamil Nadu, India.

Rajvikram Madurai Elavarasan[3], Clean and Resilient Energy Systems Laboratory, Texas A&M University, Galveston, TX 77553, USA.

Email: palpandianm@gmail.com, rajvikram787@gmail.com.

Received: Accepted: Published online:

Summary: The Photovoltaic (PV) module subjected to partial shading exhibits multiple peaks in the power-voltage characteristics leading to mismatch losses. This loss is a function of module interconnection, shading area and shading pattern. The hybrid configuration has found to be superior to improve the performance of the PV array during partial shading conditions. This work aims to minimize the mismatch loss by using an optimized jigsaw puzzle based reconfiguration technique. The physical position of the modules is rearranged based on the jigsaw puzzle pattern without altering the electrical connections. The performance of the proposed jigsaw puzzle pattern is configured on different interconnection schemes like total-cross-tied, series-parallel total-cross-tied, bridge-link total-cross-tied and honey comb total-cross-tied. For the different shading patterns, the performance

of the proposed reconfiguration technique is compared with the existing puzzle based reconfiguration technique schemes such as ken-ken, skyscraper, odd-even and latin square in terms of global maximum power point, power loss, mismatch loss, fill factor, execution ratio and performance enhancement ratio. To validate the results, the performance of the proposed reconfiguration technique is tested in MATLAB/Simulink environment and experiment setup for a 4x4 PV array. The proposed jigsaw puzzle based reconfiguration technique mitigates the occurrence of multiple local power point on the power-voltage characteristics. Hence, the simulation results show the proposed jigsaw based reconfiguration technique improves the output power by 14.01% compared to the existing reconfiguration technique under partial shaded conditions. The effectiveness of the jigsaw puzzle arrangement is also validated experimentally and the results are presented in this paper.

Keywords: Partial shading condition, hybrid configuration, jigsaw puzzle pattern, global maximum power point, performance ratio.

1 Introduction

The gap between energy generation and demand has widened due to the depletion of natural energy sources and rapidly increasing energy demand. India is the second-largest country in terms of the population having a diverse economy and energy consumption profile. For developing countries like India, energy demand is the primary concern for sustainable development. To meet the energy demand, India has doubled its renewable energy installation in the last five years [1]. International bodies related to the energy crisis and climate change has insisted all the countries increase their renewable energy capacity. Globally the contribution of renewable energy generation has increased by 26% with a major share of 64% in the total electricity generation. Hence, in recent years the contribution of renewable energy source has increased compared to coal and natural gas [2]. Among the possible renewable energy sources, the solar energy-based power generation system is found to be a simple installation, pollution-free, long life and less maintenance. Photovoltaic (PV) has become familiar due to the reduction in the price of the module and government subsidies [3].

The PV cells are connected in the string to form a module and the modules are grouped to form an array. The performance of the PV module relies on temperature, irradiation, partial shading, ageing and potential induced degradation etc., [4-6]. Among these parameters, temperature and irradiation are the dominant factors. Under the standard test condition (STC), the PV array produces a single maximum power point (MPP) on the power-voltage (P-V) characteristics. The conventional maximum power point tracking (MPPT) controller [7, 8] can track this MPP.

During the partial shading condition (PSC), the PV array produces multiple peaks on the P-V characteristics due to shading of trees, chimneys, passing cloud, dust and bird droppings etc.,[9]. This can be avoided by introducing a bypass diode, which produces multiple peaks on P-V characteristics can mislead the conventional MPPT controller and soft computing based MPPT controllers are found to be efficient in tracking the global maximum power point (GMPP) [9, 10]. During the PSC, mismatch loss (ML) occur due to the non-linear characteristics of the PV module and results in a reduction in efficiency of the PV array [11, 12].

The ML can be minimized by adopting an MPPT controller, converter topology and interconnection schemes. Various interconnection schemes are discussed in [13-15]. In this study, the PV array interconnection schemes are employed to improve the GMPP

during PSCs. To resolve these problems, PV array interconnection schemes are discussed in the literature. Under the STC, series-connected modules in the array produce the maximum power. However, under PSCs, the modules are grouped to improve the performance [16]. According to the literature, the conventional interconnection schemes namely series-parallel (SP), total-cross-tied (TCT), bridge-link (BL), honey comb (HC) are used to achieve the maximum power and to improve the GMPP. In the SP array, the PV modules are grouped to meet the load requirement. In the TCT array, the ties are connected across the rows of the junction. In the BL array, the modules are connected in bridge rectifier architecture, with the modules are connected in series to obtain the required voltage and connected in parallel to obtain the required current. In the HC array, the modules are connected in a hexagon structure, which combines the advantages of TCT and BL [17-19].

The author of [20] conducted a comprehensive study of interconnection schemes namely series, parallel, SP, TCT, BL and HC configurations under moving irradiation conditions. The result shows that the TCT configuration has provided superior results compared to other interconnection schemes. The author of [21] investigated the interconnection scheme using a Genetic Algorithm under different PSCs. The author concluded that the Genetic Algorithm has provided improved performance than the conventional interconnection schemes. The author of [22] compared the SP configuration to the TCT and BL configuration under PSCs. The author found that there is no optimum configuration since the performance of the array relies on the shading pattern. From the literature, it is understood that the TCT configuration has yielded superior results under PSCs. The main drawback of the TCT configuration, when the modules connected in the rows are partial shading leads to the reduction of output power. In addition, the ties connected across the rows of the junction in the TCT configuration causes more power loss. The BL configuration has more numbers of series-connected modules and has more power loss (PL) compared to the TCT configuration. The HC configuration has more numbers of series-connected modules and has more PL compared to TCT and BL configuration. To overcome this problem, the reconfiguration technique is anticipated.

The reconfiguration technique aims to distribute the effects of partial shading uniformly throughout the array to minimize the ML[23]. The author of [24] compared the Sudoku based TCT interconnection with the conventional total-cross-tied (CTCT) configuration. Here, the position of the modules is rearranged based on the Sudoku pattern without altering the electrical connection. The author reported that the Sudoku based interconnection scheme has yielded improved results. The author of [25, 26] compared the rearranged total-cross-tied (RTCT) configuration with CTCT and found that the RTCT configuration has yielded superior results in terms of PL and fill factor (FF). The author of [27] proposed a 4×4 Magic Square puzzle pattern to rearrange the module within the array. The author concluded that the proposed pattern has improved the GMPP under most PSCs. The author of [28] proposed a Zigzag technique, to rearrange the location of the modules within the PV array based on the proposed technique to reduce PL and improve FF. The mathematical analysis of the HC configuration is analyzed in [29]. The author of [30] proposed a two-phase method for rearranging the position of the modules in the PV array and compared with TCT, partial swarm optimization and Sudoku configurations for improving the power. However, it is necessary to explore the hybrid configuration with a recent and effective reconfiguration technique in a realistic

environment. From the literature, it is concluded that the reconfiguration technique has improved the GMPP and reduced local MPP on the P-V characteristics, but these configurations have certain limitations. The effectiveness of the reconfiguration depends on the ability to distribute the effects of partial shading uniformly throughout the array. To overcome this complexity, the hybrid configuration is anticipated.

The hybrid PV array configurations are obtained by combining the advantages of two configurations namely SPTCT, BLTCT and HCTCT. The author considered only the shading pattern like progressively horizontal, progressively vertical and progressively diagonal [27]. The efficacy of hybrid bridge-link total-cross-tied (BLTCT) configuration over SP, TCT, BL and hybrid series-parallel total-cross-tied (SPTCT) configurations are analyzed in [27, 31-33]. The reduction of ties in the hybrid configuration reduces wiring losses and complexity of the PV system. From the literature review, it is evidence that the hybrid PV array configuration is found to be a better solution for diluting the concentration of the partial shading effects and extracting the maximum power. However, the performance of the hybrid PV array configuration relies on the effectiveness of the reconfiguration technique to disperse throughout the array. Hence, it is necessary to explore the effective reconfiguration technique on hybrid PV array configuration schemes to dilute the concentration of the partial shading effects thereby extracting more output power from the PV array.

This study presents a reconfiguration technique to rearrange the position of the modules of the 4x4 PV array to improve the output power under the PSCs. The contribution of the proposed study are as follows:

- After the investigation, it is found that the jigsaw (JS) puzzle pattern can effectively rearrange the position of the modules within the PV array without altering the electrical connection. Hence, the concentration of the partial shading is diluted by dispersing the shading effects throughout the array.
- To enhance the maximum power of TCT and hybrid configurations such as SPTCT, BLTCT, and honey comb total-cross-tied (HCTCT) configurations are rearranged according to the JS puzzle pattern.
- The JS puzzle pattern mitigates the occurrence of local MPP in the P-V characteristics and avoids the need for an MPPT controller to track the GMPP.
- The mathematical analysis of the hybrid configuration is derived for better understanding.
- To validate the effectiveness of the JS puzzle based reconfiguration technique, its performance is compared with existing reconfiguration techniques like ken-ken (KK) [34], Skyscraper (SS) [34], odd-even (OE) [35] and latin square (LS) [36] to overcome the following shortcomings.
- In Reference [34], the author proposed KK and SS puzzle pattern for a 4x4 TCT array to enhance the maximum power during the PSCs. The shortcoming of this work: The PSCs considered for the study, most of the modules receives full irradiation (1000W/m^2).
- In Reference [35], the author proposed the OE puzzle pattern for a 4x4 TCT array to enhance the maximum power during the PSCs. The shortcoming of this works: If the row or column is partially

shaded, it rearranged in two rows only, thus the shading effects are not uniformly distributed throughout the array.

- In Reference [36], the author proposed LS puzzle pattern for a 4x4 TCT array to extract the maximum power during the PSCs. The shortcomings of this work: If the first column remains unaltered if the first column is shaded it results in the reduction of output power. If the modules connected in the first row is rearranged in the diagonal results in the reduction of output current.
- The performance of the various configurations is analyzed in terms of GMPP, PL, ML, FF, execution ratio (ER) and performance enhancement ratio (PE).
- The effectiveness of the JS and existing puzzle arrangements is validated experimentally on the TCT and hybrid configurations.

This work is organized as follows. Section 2 presents the mathematical modelling of the PV array. Section 3.1 discussed the formation of JS puzzle and pattern arrangements. Section 3.2 describes the physical relocation of modules in an array according to the JS puzzle pattern. Section 3.3, describes the mathematical analysis of the hybrid configuration. In Section 3.4, a description of the existing puzzle pattern considered for the investigation. In Section 3.5 description of partial shading pattern. In Section 3.6, a description of the performance parameter considered to validate the performance. Section 4 results and discussion of various configuration under PSCs and Section 5 describes the experimental verification of the proposed puzzle arrangements along with conclusion in Section 6.

2 Mathematical Model of PV Array

The single-diode PV model developed in [37] has been designed in MATLAB Simulink environment. The equivalent circuit of the single-diode PV cell comprises a current source connected in anti-parallel with diode, series (R_s) and shunt resistance (R_{sh}).

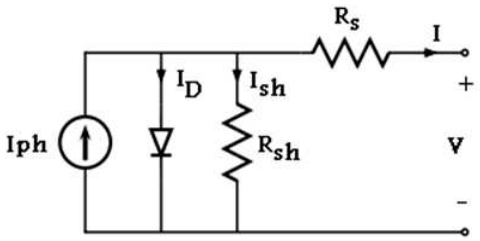

Fig. 1 Single diode PV cell

Apply kirchhoff's current law for the PV cell model shown in Fig. 1. The PV cell current is given in equation (1).

$$I = I_{Ph} - I_D - I_{sh} \quad (1)$$

Where I_{ph} is photo-current linearly depends on incident irradiation, I_D is responsible for the non-linearity of the PV cell, I_{sh} is the shunt current of the PV cell. Therefore, the PV cell current is derived as shown in Equation (2).

$$\boldsymbol{I = I_{Ph} - I_o\left[exp\left(\frac{q(V+IR_s)}{akT}\right) - 1\right] - \frac{V+IR_s}{R_{sh}}} \quad (\mathbf{2})$$

Where I_o is the saturation current of the diode, k is the Boltzmann constant and its value is 1.3806503×10^{-23} J/K, q is the electron charge (1.602×10^{-19} C), T is the cell temperature and a is the ideality constant.

The PV cells are connected in series to form a PV module and series-connected PV cells are represented as series-connected cells (N_{se}). The module current (I_m) in terms of the module voltage (V_m) with N_{se} cells connected in series. The module current is represented in Equation (3).

$$I_m = I_{ph} - N_p I_o \left[exp\left(\frac{q(V_m + R_s I_m)}{N_{se} akT} \right) - 1 \right] - \frac{V_m + R_s I_m N_{se}}{N_{se} R_{sh}} \quad (3)$$

The PV cells are connected in series to form a module and modules are connected in series and parallel to form a PV array to meet the load requirement. Fig. 2 shows the equivalent circuit of the PV array with series (N_s) and parallel (N_p) connected modules. The PV array current (I_a) in terms of array voltage (V_a) is represented in Equation (4).

$$I_a = N_p I_{ph} - N_p I_o \left[exp\left(\frac{q\left(V_a + R_s I_a \frac{N_s}{N_p}\right)}{N_s akT} \right) - 1 \right] - \frac{V_a + R_s I_a \frac{N_s}{N_p}}{\frac{N_s}{N_p} R_{sh}} \quad (4)$$

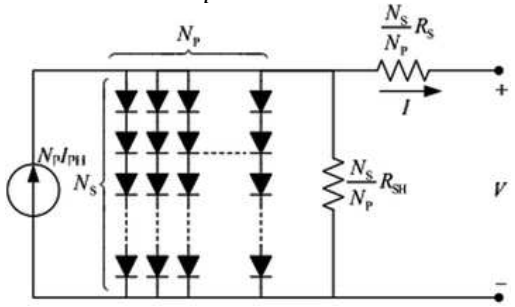

Fig. 2 Equivalent circuit of PV array

The mathematical model of the PV module is obtained with the electrical parameters of the module Kyocera KC200GT is represented in Table 1. A bypass diode is connected in anti-parallel with each module to provide an alternate path under PSC within a series-connected string.

Table 1 Electrical characteristics of the PV module at STC (1000 W/m^2, 25°C).

Electrical characteristics	Ratings
Maximum Power (P_{max})	200W
Open circuit voltage (V_{oc})	32.9V
Voltage at maximum power (V_{mpp})	26.3V
Short circuit current (I_{sc})	8.21A
Current at maximum power (I_{mpp})	7.61A
Temperature coefficient of V_{oc}	-1.23×10^{-1} V/°C
Temperature coefficient of I_{sc}	3.18×10^{-3}A/°C
Number of cells connected in series (N_s)	54
Series resistance (R_s)	0.221 Ω
Parallel resistance (R_{sh})	415.405 Ω
Ideality factor (a)	1.3

3 Methodology

3.1 Formation of proposed jigsaw puzzle arrangement

In this study, a JS puzzle pattern is proposed for rearranging the position of the modules within the 4x4 PV array to mitigate the ML under PSCs. A JS puzzle consists of m x n grid, which is similar to an ordinary Sudoku puzzle. In JS puzzle, the squares are irregular in shape and each of the squares is represented by bold lines. This puzzle places the numbers from 1 to N in the m x n grid, without duplicating the same number in the row or column. Fig. 3a shows the 4x4 JS puzzle pattern, which consists of 16 blocks, constitute of four rows and columns. The puzzle consists of four irregular squares, in which each square has the numbers from 1 to 4 without duplicating the same number in a row or column. The procedure for filling the empty square is as follows.

Step 1: Square 1 has the number 1 and 3, which can be filled by 2, 4 in Fig. 3b and the first row of block 2 is filled with 1 as depicted in Fig. 3c.

Step 2: The remaining blocks of square 2 are filled with 2, 3 and square 3 on the first column with 3 as depicted in Fig. 3d.

Step 3: Similarly, square 4 is filled with 1 and 4 as depicted in Fig. 3e. Similarly, fill the remaining squares as depicted in Fig. 3f. Fig. 3g

shows the pattern arrangement of the puzzle has to be considered for further analysis. In the puzzle pattern, the first digit represents the position of the module and the second digit represents the column number. For example in module 21, 2 represents the position of the module and 1 represents the column number. In the PV array, the position of the modules is rearranged according to the JS puzzle pattern without altering the electrical connection.

3.2 Physical relocation of modules in the PV array

The puzzle arrangement of the proposed JS reconfiguration technique is represented in Fig. 3f. This work aims to rearrange the position of the modules within the array according to the JS puzzle pattern. Fig. 4 (a-d) shows the CTCT, SPTCT, BLTCT and HCTCT configurations considered for the analysis.

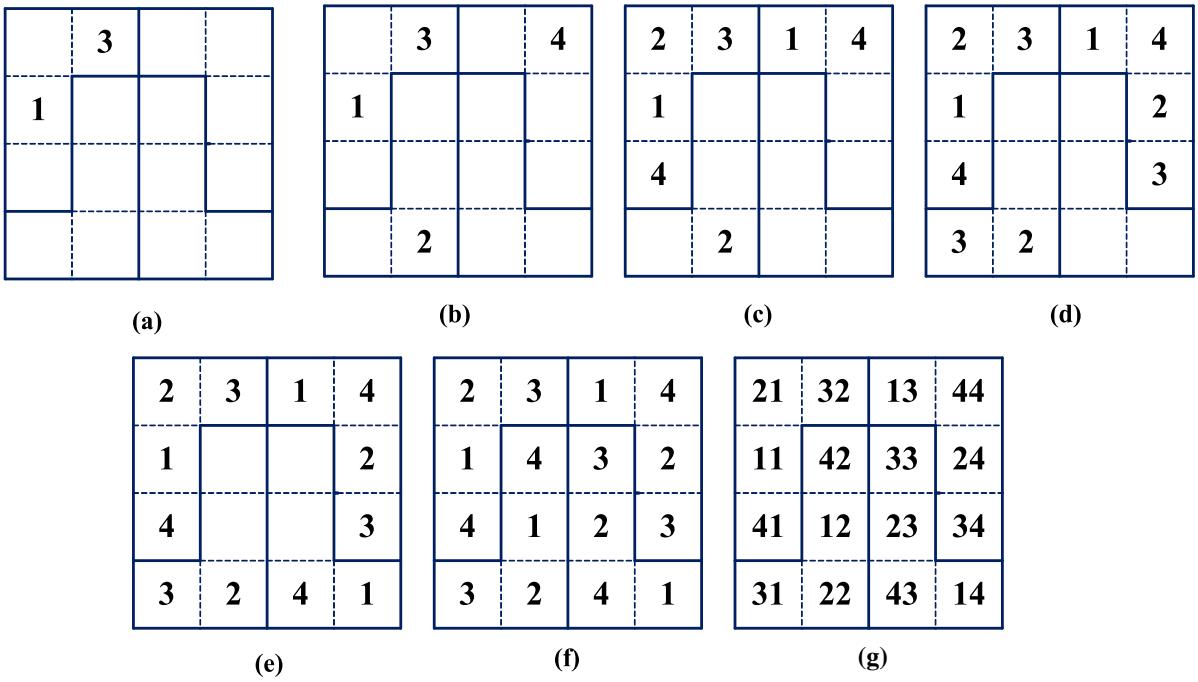

Fig. 3 a - g JS puzzle pattern

Fig. 5 (a-d) shows the RTCT, rearranged series-parallel total-cross-tied (RSPTCT), rearranged bridge-link total-cross-tied (RBLTCT) and rearranged honey-comb total-cross-tied (RHCTCT) configurations which are rearranged according to the proposed JS arrangement for dispersing the shading effects uniformly throughout the array.

3.3 Mathematical analysis of the PV array configurations

The mathematical analysis of the TCT and hybrid configurations is derived for better understanding. The expression for the voltage, current and power of the TCT and hybrid configuration is derived as follows:

3.3.1 TCT PV array configuration

The TCT configuration is derived from the SP configuration by connecting ties across the rows of the junction. The array current is the sum of the current produced by the modules connected in a row. The row voltage is equal to the open-circuit voltage of the single module. The array voltage is the sum of the voltage across all rows[38]. The current flowing through each module and voltage across each module in the TCT configuration is represented in Fig. 6. The array voltage, current and power of the TCT configuration is given by the following equation.

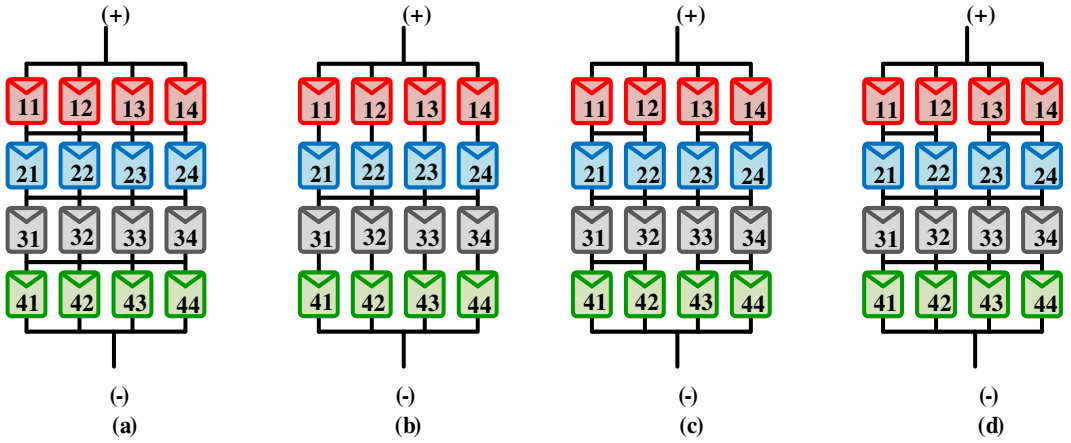

Fig. 4 PV configuration **a** CTCT, **b** SPTCT, **c** BLTCT, **d** HCTCT

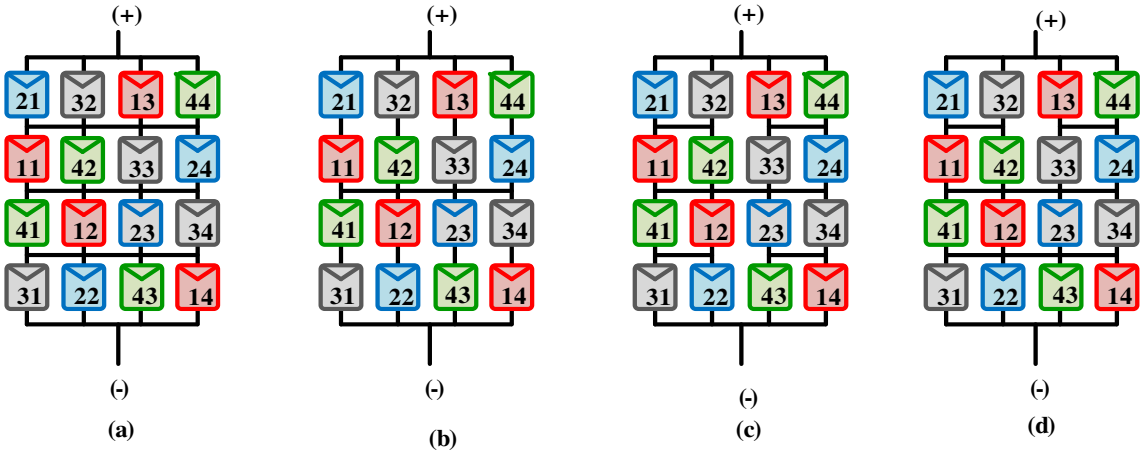

Fig. 5 JS puzzle pattern for **a** RTCT, **b** RSPTCT, **c** RBLTCT, **d** RHCTCT

$$I_{array} = iI_{string} = 4I_m \quad (5)$$

$$V_{array} = jV_{string} = 4V_m \quad (6)$$

$$P_{array} = (V_{array})(I_{array}) = 16V_mI_m \quad (7)$$

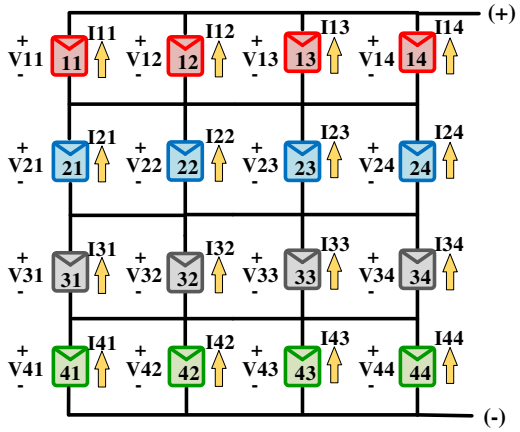

Fig. 6 Mathematical analysis of TCT configuration

Where i is the number of modules connected in parallel in a string and j is the number of strings connected in series.

3.3.2 SPTCT PV array configuration

The SPTCT configuration is the combination of SP and TCT configuration. In SPTCT configuration, rows are cross-linked at every alternate row. This has a lesser number of interconnection compared to BLTCT and HCTCT. However, SPTCT generates less power than hybrid configurations[39]. The current flowing through each module and voltage across

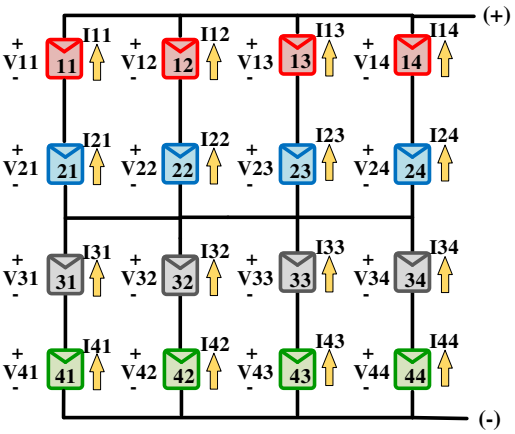

Fig. 7 Mathematical analysis of SPTCT configuration

each module in the SPTCT configuration is represented in Fig. 7. The array voltage, current and power of the SPTCT configuration is given by the following equation.

$$I_{array} = I_{11} + I_{12} + I_{13} + I_{14} = 4I_m \quad (8)$$

$$V_{array} = \sum_i^4 V_i = 4V_m \quad (9)$$

$$P_{array} = (V_{array})(I_{array}) = 16V_m I_m \quad (10)$$

Where i is the row of the PV array.

3.3.3 BLTCT PV array configuration

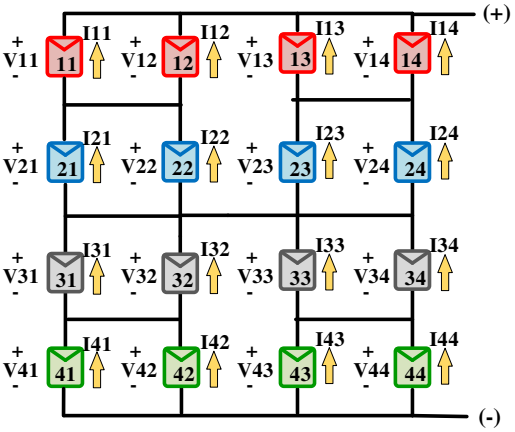

Fig. 8 Mathematical analysis of BLTCT configuration

The BLTCT configuration is the combination of BL and TCT configuration. This configuration is an alternative to TCT configuration, which can be obtained by reducing the number of ties connected among the modules. Hence, the stress on the PV module is minimized [40]. The current flowing through each module and voltage across each module in BLTCT configuration is represented in Fig. 8. The array voltage, current and power of the BLTCT configuration is given by the following equation.

$$I_{array} = I_{11} + I_{12} + I_{13} + I_{14} = 4I_m \quad (11)$$

$$V_{array} = \sum_i^4 V_i = 4V_m \quad (12)$$

$$P_{array} = (V_{array})(I_{array}) = 16V_m I_m \quad (13)$$

Where i is the row of the PV array.

3.3.4 HCTCT PV array configuration

The HCTCT configuration is the combination of HC and TCT configuration. In HC configuration, the first and second rows are connected in HC structure and the third and fourth tow are connected on the TCT configuration. The number of the parallel-connected module in a row is high compared to the BLTCT [29]. The current flowing through each module and voltage across each module in the HCTCT configuration is represented in Fig. 9. The array voltage, current and power of the HCTCT configuration is given by the following equation.

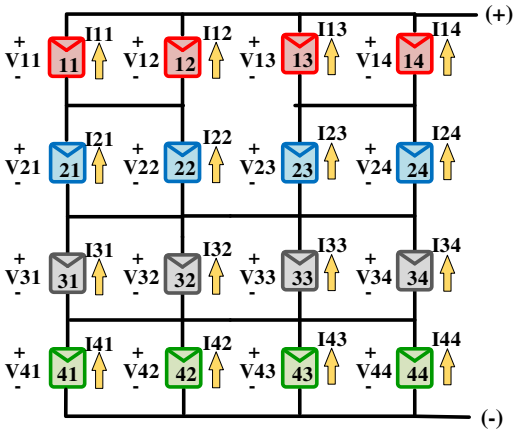

Fig. 9 Mathematical analysis of HCTCT configuration

$$I_{array} = I_{11} + I_{12} + I_{13} + I_{14} = 4I_m \quad (14)$$

$$V_{array} = \sum_i^4 V_i = 4V_m \quad (15)$$

$$P_{array} = (V_{array})(I_{array}) = 16V_m I_m \quad (16)$$

Where i is the row of the PV array.

3.4 Description of the existing puzzle patterns

The conventional 4x4 PV array is rearranged according to the proposed JS puzzle pattern as depicted in Fig. 4 (a-d) & Fig. 5 (a-d). To investigate the effectiveness of the proposed puzzle pattern comparison is made with the RTCT, RSPTCT, RBLTCT and RHCTCT. The I-V and P-V characteristics of these rearranged configurations have been modelled in the MATLAB/Simulink environment are utilized for comparing the performance of the proposed puzzle pattern under PSCs. A comparison has also been made with existing reconfiguration techniques namely KK, SS, OE and LS in mitigating the ML under PSCs. All these configurations are illustrated in Fig. 10 (a-d).

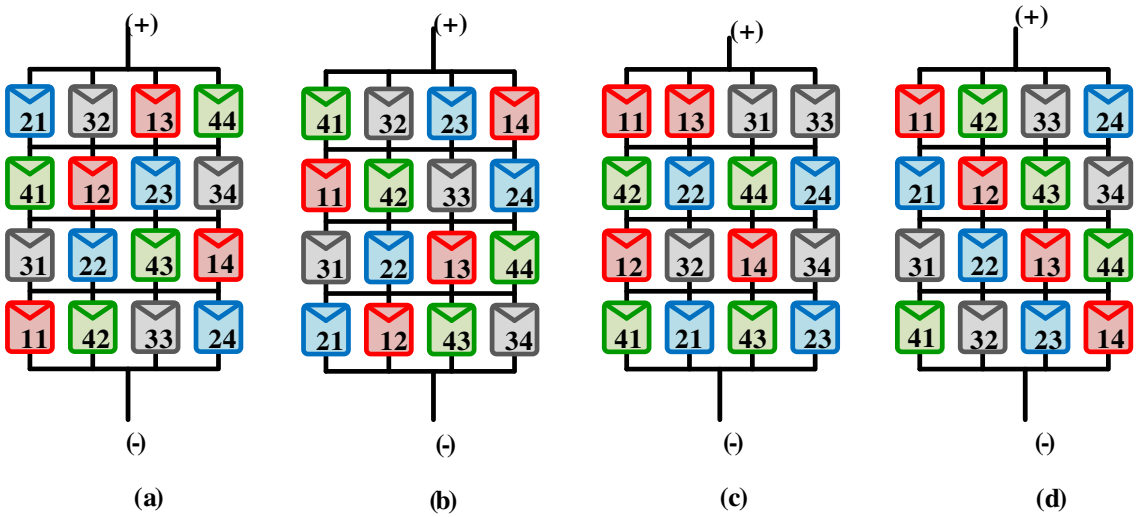

Fig. 10 Existing puzzle pattern **a** KK, **b** SS, **c** OE **d** LS.

Under uniform irradiation condition, all the 4x4 PV array configuration produces a maximum power of 3200 W. During the PSCs, the output power generated by the PV array decreases due to ML. To mitigate the ML, the PV array is rearranged with a hybrid combination. This hybrid interconnection yields superior results than the CTCT interconnection during PSCs. The JS puzzle pattern is applied to the hybrid interconnection to rearrange the physical location of the module within the array. Hence, the concentration of the shading is reduced and thereby distributing the shading effects throughout the array.

3.5 Partial shading scenario

In this study, the effectiveness of the JS puzzle pattern is verified by comparing the performance of the different conventional and hybrid configurations under PSCs. Four types of shading conditions namely short narrow, short wide, long narrow and long wide are considered. Under the PSCs, it is assumed that the shaded module receives irradiation of 100 W/m^2, 200 W/m^2, 300 W/m^2, 400 W/m^2, 500 W/m^2 and the unshaded module receives irradiation of 1000 W/m^2.

This type of shading conditions is applied to the 4x4 JS pattern. The partial shading dispersion effect on the JS puzzle pattern is applied under different configurations. Similarly, the partial shading dispersion effect is applied to the existing KK, SS, OE, and LS patterns. The performance of the existing and JS puzzle pattern is analyzed in terms of PL, ML, FF, ER and PE.

3.5.1 Case 1 Short narrow

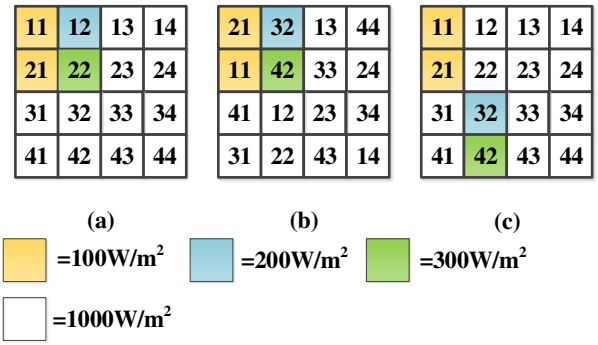

Fig. 11 Partial shading pattern in case 1 short narrow **a** TCT configuration, **b** JS configuration, **c** Partial shading dispersion with JS puzzle arrangement

For case 1 short narrow shading pattern is created with the shaded module receives three different irradiation of 100 W/m^2, 200 W/m^2, 300 W/m^2 and the unshaded module receives irradiation of 1000 W/m^2 as depicted in Fig. 11. This type of shading conditions is applied to the 4x4 PV array configuration constructed for the short narrow condition.

3.5.2 Case 2 Short wide

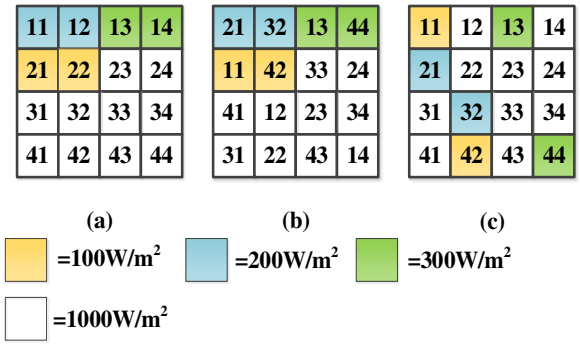

Fig. 12 Partial Shading pattern in case 2 short wide **a** TCT configuration, **b** JS configuration, **c** Partial shading dispersion with JS puzzle arrangement

For case 2 short wide shading pattern is created with the shaded module receives three different irradiation of 100 W/m^2, 200 W/m^2, 300 W/m^2 and the unshaded module receives irradiation of 1000 W/m^2 depicted in Fig. 12. From Fig. 12, it is clear that the impact of shading on the PV array is increased, results in a reduction of maximum power.

3.5.3 Case 3 Long narrow

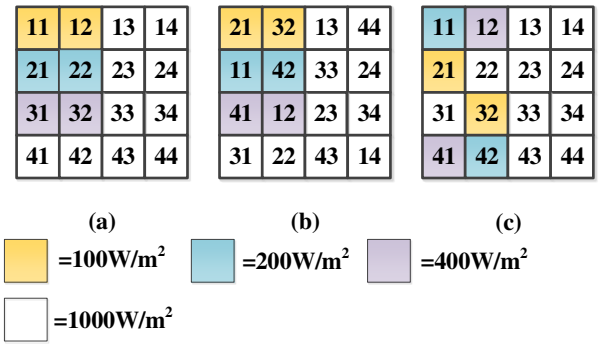

Fig. 13 Partial shading pattern in case 3 long narrow **a** TCT configuration, **b** JS configuration, **c** Partial shading dispersion with JS puzzle arrangement

For case 3 long narrow shading pattern is created with the shaded module receives three different irradiation of 100 W/m^2, 200 W/m^2, 400 W/m^2 and the unshaded module receives irradiation of 1000 W/m^2 as depicted in Fig. 13. From Fig. 13 it is understood that the impact of shading on more number of rows increased as compared to short narrow conditions.

3.5.4 Case 4 Long wide

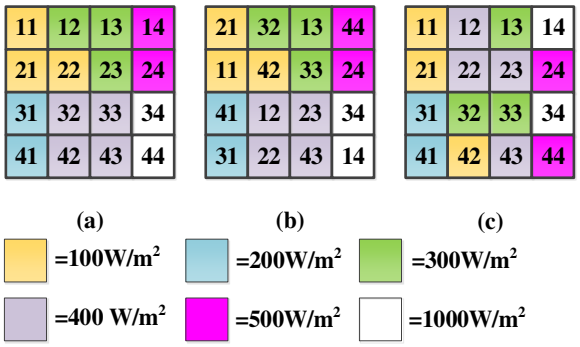

Fig. 14 Partial shading pattern in case 4 long wide **a** TCT configuration, **b** JS configuration, **c** Partial shading dispersion with JS puzzle arrangement

For the case 4 long wide shading pattern is created with the shaded module receives five different irradiation of 100 W/m^2, 200 W/m^2, 300 W/m^2, 400 W/m^2 and 500 W/m^2 the unshaded module receives irradiation of 1000 W/m^2 as depicted in Fig. 14. From Fig. 14, it is

clear that the impact of shading is increased as compared to other shading conditions.

3.6 Performance parameter

3.6.1 Power loss

The power loss is the ratio of GMPP at STC and PSC to the GMPP at STC.

$$PL = (G_{MPP}\ at\ STC - G_{MPP}\ at\ PSC)/G_{MPP}\ at\ STC \quad (17)$$

3.6.2 Mismatch loss

ML refers to the difference in power between STC and PSC.

$$ML = G_{MPP}at\ STC - G_{MPP}\ at\ PSC \quad (18)$$

3.6.3 Fill factor

The fill factor is the squareness of the I-V curve. In STC, the I-V characteristics curve is rectangular, under PSC it deviates from its shape. As the FF is close to unity, PV array performance is higher. Hence, it is defined as the ratio of maximum power under PSC to the power generated.

$$FF = \frac{V_{mp} \times I_{mp}\ at\ PSC}{V_{oc} \times I_{sc}} \quad (19)$$

3.6.4 Execution ratio

The execution ratio is defined as the ratio of GMPP at PSC to GMPP at STC.

$$ER\ (\%) = \frac{G_{MPP}\ at\ PSC}{G_{MPP}\ at\ STC} \quad (20)$$

3.6.5 % Performance Enhancement ratio compared to the conventional configuration

% performance enhancement is defined as the ratio of the difference in power between GMPP at STC. and PSCs.

$$\%\ PE = \frac{P_{GMPP}\ (Proposed, KK, SS, OE, LS) - P_{GMPP}(TCT, SPTCT, BLTCT, HCTCT)}{P_{GMPP}\ (Proposed,\ KK,\ SS, OE, LS)} \quad (21)$$

4 Results and Discussion

4.1 Case 1 Short narrow

The performance analysis of JS puzzle pattern with short narrow shading condition in comparison with the conventional (TCT, SPTCT, BLTCT, HCTCT) configurations and rearranged hybrid configurations of KK, SS, OE and LS puzzle pattern is made. The result in the form of GMPP, PL, ML, FF, ER and PE is presented in Table 2.

4.1.1 TCT configuration

Results obtained from the CTCT and RTCT configurations for the various puzzle pattern with short narrow shading condition indicates that the JS puzzle pattern performs superior and generates GMPP of 2493 W (Fig. 15a). The GMPP of the KK puzzle pattern is very close to the JS puzzle pattern with a GMPP of 2490 W. The SS, LS, OE and CTCT follows the performance by 2120 W, 2119 W, 2043 W and 2005 W. In the TCT configuration, since the ties are connected across the junction, the obtained GMPP is based on the effectiveness of the puzzle pattern. Hence, the JS puzzle pattern of TCT configuration has generated relatively higher maximum power output power under short narrow condition.

From Table 2, it is observed that the JS puzzle pattern has an ER ratio of 77.90%, followed by the KK, SS, LS, OE and CTCT by 77.80%, 66.24%, 66.23%, 63.84% and 62.66%. Also, the JS puzzle pattern has a PE ratio of 19.58% in comparison with the CTCT, followed by the KK, SS, LS and OE of 19.49%, 5.43%, 5.41% and 1.87% respectively.

4.1.2 SPTCT configuration

Results obtained from the conventional series-parallel total-cross-tied (CSPTCT) and RSPTCT configurations for the various puzzle pattern with short narrow shading condition indicates that the JS puzzle pattern performs superior and generates GMPP of 2487 W (Fig. 15b). The LS, CSPTCT, SS, OE and KK puzzle pattern follows the performance of the JS puzzle pattern by 2033 W, 1984 W, 1954 W, 1914 W and 1874 W. Thus, it is noticed that the performance of the JS puzzle pattern generates 454 W more output power than the LS pattern. It is noticed that the JS puzzle pattern of SPTCT configuration has generated relatively higher maximum power output power under short

narrow condition. Since the SPTCT configuration has more number of series-connected modules compared to other configuration. At the time of rearranging the modules according to the various puzzle pattern, the shaded modules are connected in series thereby reducing the output power of the PV array.

From Table 2, it is observed that the JS puzzle pattern has an ER ratio of 77.71%, followed by the LS, CSPTCT, SS, OE and KK puzzle pattern of 63.55%, 62.00%, 61.05%, 59.81% and 58.57%. Also, the JS puzzle pattern has a PE ratio of 20.22% in comparison with CSPTCT, followed by the LS of 2.43%. The SS, OE and KK have a reduction in the PE ratio by -1.56%, -3.66%, and -5.85%, in comparison with the CSPTCT.

Table 2. Simulation results for case 1.

Short Narrow	Puzzle Pattern	V_{mp} (V)	I_{mp} (A)	GMPP (W)	PL (%)	ML (W)	FF (%)	ER (%)	PE (%)
TCT	CTCT	18.27	109.66	2005	37.34	1195.00	46.84	62.66	NA
	KK	24.22	102.77	2490	22.20	710.33	58.16	77.80	19.49
	SS	19.19	110.45	2120	33.76	1080.34	49.52	66.24	5.43
	OE	18.23	112.07	2043	36.16	1157.26	47.72	63.84	1.87
	LS	19.24	110.17	2119	33.77	1080.70	49.51	66.23	5.41
	JS	23.99	103.92	2493	22.10	707.30	58.23	77.90	19.58
SPTCT	CSPTCT	18.09	109.66	1984	38.00	1216.02	46.35	62.00	NA
	KK	17.78	105.41	1874	41.43	1325.62	43.79	58.57	-5.85
	SS	18.25	107.03	1954	38.95	1246.43	45.64	61.05	-1.56
	OE	23.84	80.30	1914	40.19	1286.04	44.71	59.81	-3.66
	LS	18.91	107.53	2033	36.45	1166.53	47.50	63.55	2.43
	JS	23.93	103.92	2487	22.29	713.26	58.09	77.71	20.22
BLTCT	CBLTCT	18.15	109.66	1991	37.79	1209.29	46.50	62.21	NA
	KK	23.52	105.41	2479	22.53	720.90	57.91	77.47	19.70
	SS	18.66	109.66	2046	36.07	1154.10	47.79	63.93	2.70
	OE	18.51	109.44	2026	36.70	1174.27	47.32	63.30	1.73
	LS	19.07	107.53	2051	35.91	1149.06	47.91	64.09	2.94
	JS	23.97	103.92	2491	22.15	708.81	58.19	77.85	20.09
HCTCT	CHCTCT	18.15	109.66	1991	37.79	1209.29	46.50	62.21	NA
	KK	23.54	105.41	2482	22.45	718.32	57.97	77.55	19.78
	SS	19.16	110.28	2113	33.97	1087.13	49.36	66.03	5.78

Short Narrow	Puzzle Pattern	V_{mp} (V)	I_{mp} (A)	GMPP (W)	PL (%)	ML (W)	FF (%)	ER (%)	PE (%)
	OE	18.54	109.44	2029	36.59	1170.73	47.40	63.41	1.90
	LS	18.66	110.17	2056	35.76	1144.26	48.02	64.24	3.16
	JS	23.99	103.92	2493	22.10	707.30	58.23	77.90	20.14

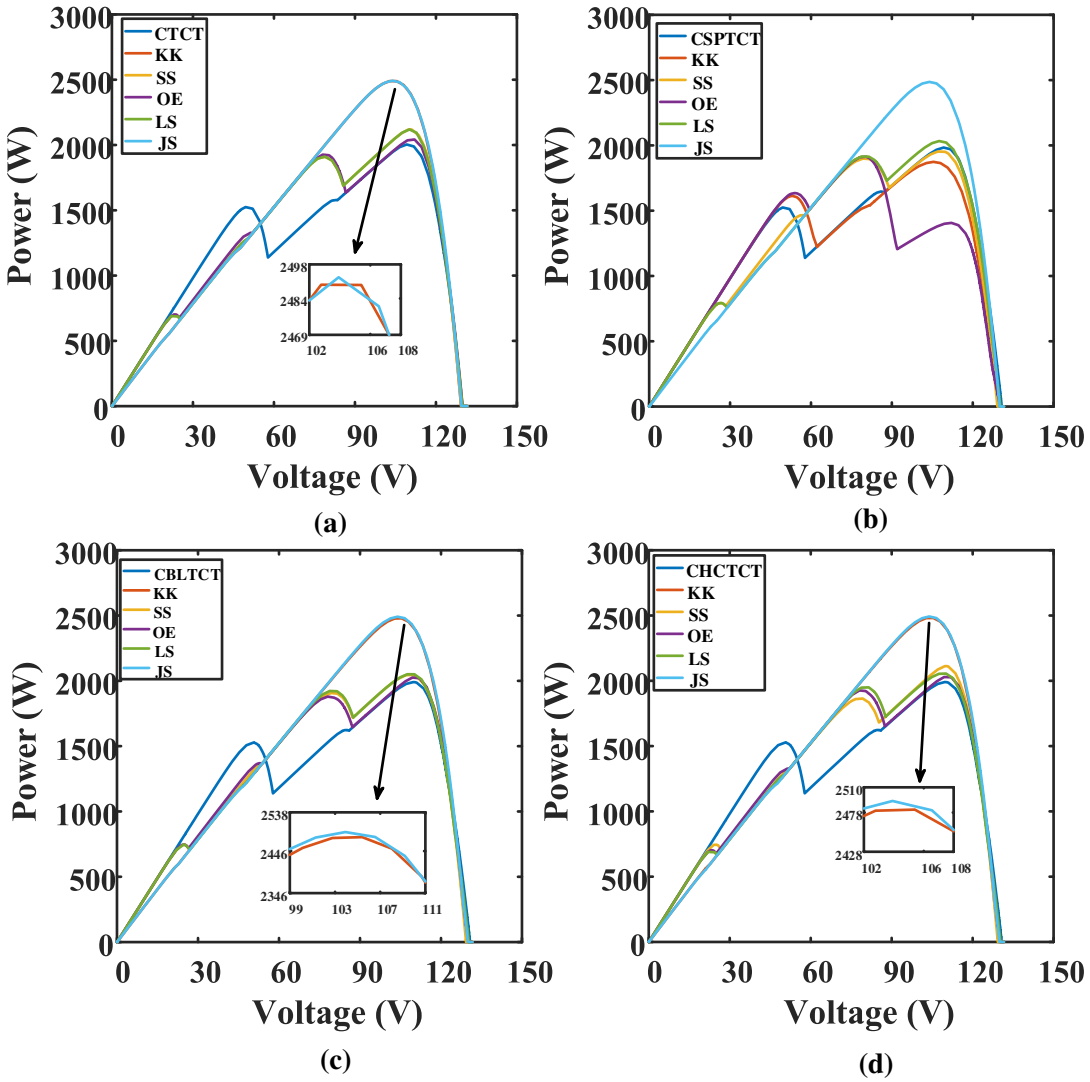

Fig. 15 P-V characteristics: **a** TCT configuration, **b** SPTCT configuration, **c** BLTCT configuration, **d** SPTCT configuration for case 1

4.1.3 BLTCT configuration

Results obtained from the conventional bridge-link total-cross-tied (CBLTCT) and RBLTCT configurations for the various puzzle pattern with short narrow shading condition indicates that the JS puzzle pattern performs superior and generates GMPP of 2491 W (Fig. 15c). The GMPP of the KK is very close to the JS puzzle pattern with a GMPP of 2479 W. The LS, SS, OE and CBLTCT pattern follows the performance by 2051 W, 2046 W, 2026 W and 1991 W. Hence, it is noticed that the JS puzzle pattern of BLTCT configuration generates relatively higher maximum power output power

under short narrow condition. Here, the number of parallel-connected modules in a row is reduced compared to TCT configuration and hence the maximum power is reduced.

From Table 2, it is observed that the JS puzzle pattern has an ER ratio of 77.85%, followed by the KK, LS, SS, OE and CBLTCT pattern by 77.47%, 64.09%, 63.93%, 63.30% and 62.21%. Also, the JS puzzle pattern has a PE ratio of 20.09% in comparison with the C-BLTCT, followed by the KK, LS, SS, OE and CBLTCT pattern by 19.70%, 2.94%, 2.70% and 1.73% respectively.

4.1.4 HCTCT configuration

Results obtained from the conventional honey-comb total-cross-tied (CHCTCT) and RHCTCT configurations for the various puzzle pattern with short narrow shading condition indicates that the JS puzzle pattern performs superior and generates GMPP of 2493 W (Fig. 15d). The GMPP of the KK is very close to the JS puzzle pattern with a GMPP of 2482 W. The SS, LS, OE and CHCTCT pattern follows the performance by 2113 W, 2056 W, 2029 W and 1991 W. Thus, it is noticed that the JS puzzle pattern of HCTCT configuration has generated relatively higher maximum power output power under short narrow condition. Here, the number of parallel-connected modules in a row is high compared to the BLTCT and hence the obtained GMPP is improved.

From Table 2, it is observed that the JS puzzle pattern has an ER ratio of 77.90%, followed by the KK, SS, LS and OE and CHCTCT by 77.55%, 66.03%, 64.24%, 63.41% and 62.21%. Also, the JS puzzle pattern has a PE ratio of 20.14% in comparison with the CHCTCT, followed by the KK, SS, LS and OE by 19.78%, 5.78%, 3.16%, 1.90% and 1.73% respectively.

Table 3 Simulation results for case 2.

Short Wide	Puzzle Pattern	V_{mp} (V)	I_{mp} (A)	GMPP (W)	PL (%)	ML (W)	FF (%)	ER (%)	PE (%)
TCT	CTCT	30.38	50.28	1527	52.26	1672.32	35.69	47.74	NA
	KK	18.77	107.08	2010	37.19	1190.01	46.95	62.81	24.00
	SS	18.40	106.69	1963	38.65	1236.69	45.86	61.35	22.19
	OE	18.89	108.23	2044	36.12	1155.77	47.75	63.88	25.27
	LS	18.06	108.64	1963	38.67	1237.49	45.84	61.33	22.16
	JS	18.98	105.80	2008	37.24	1191.82	46.91	62.76	23.93
SPTCT	CSPTCT	18.97	83.22	1579	50.67	1621.40	36.88	49.33	NA
	KK	30.00	52.04	1561	51.20	1638.55	36.48	48.80	-1.10
	SS	13.34	109.32	1459	54.42	1741.47	34.07	45.58	-8.23
	OE	30.23	51.69	1563	51.17	1637.39	36.50	48.83	-1.02
	LS	19.39	80.30	1557	51.33	1642.71	36.38	48.67	-1.37
	JS	18.10	105.80	1915	40.17	1285.33	44.73	59.83	17.55
BLTCT	CBLTCT	18.97	83.22	1579	50.67	1621.40	36.88	49.33	NA

Short Wide	Puzzle Pattern	V_{mp} (V)	I_{mp} (A)	GMPP (W)	PL (%)	ML (W)	FF (%)	ER (%)	PE (%)
	KK	18.50	107.08	1981	38.09	1218.73	46.28	61.91	20.32
	SS	17.64	106.69	1882	41.19	1318.01	43.96	58.81	16.12
	OE	18.35	105.60	1937	39.45	1262.53	45.26	60.55	18.52
	LS	19.79	81.21	1607	49.77	1592.51	37.55	50.23	1.80
	JS	18.74	105.80	1982	38.05	1217.68	46.31	61.95	20.37
HCTCT	CHCTCT	18.97	83.22	1579	50.67	1621.40	36.88	49.33	NA
	KK	18.63	107.08	1995	37.65	1204.69	46.61	62.35	20.88
	SS	18.18	106.69	1939	39.40	1260.85	45.30	60.60	18.59
	OE	18.15	108.23	1964	38.62	1235.69	45.89	61.38	19.64
	LS	24.43	76.01	1857	41.98	1343.25	43.37	58.02	14.98
	JS	18.86	105.80	1995	37.65	1204.85	46.61	62.35	20.88

4.2 Case 2 Short wide

4.2.1 TCT configuration

Results obtained from the CTCT and RTCT configurations for the various puzzle pattern with short wide shading condition indicates that the OE puzzle pattern performs superior and generates GMPP of 2044 W (Fig. 16a). The GMPP of the KK and JS puzzle patterns are close with the OE pattern with GMPP of 2010 W and 2008 W. The SS, LS, and CTCT pattern follow the performance by 1963 W, 1963 W and 1527 W. Thus, it is noticed that the OE puzzle pattern of TCT configuration has generated relatively higher maximum power output power under short narrow condition.

From Table 3, it is observed that the OE pattern has an ER ratio of 63.88%, followed by the KK, JS, SS, LS, and CTCT pattern by 62.81%, 62.76%, 61.35%, 61.33% and 47.74%. Also, the OE puzzle pattern has a PE ratio of 25.27% in comparison with the CTCT, followed by the KK, JS, SS and LS by 24.00%, 23.93%, 22.19%, 22.16% respectively.

4.2.2 SPTCT configuration

Results obtained from the CSPTCT and RSPTCT configurations for the various puzzle pattern with short wide shading condition indicates that the JS puzzle pattern performs superior and generates GMPP of 1915 W (Fig. 16b). The CSPTCT, OE, KK, LS and SS follows the performance by 1579 W, 1563 W, 1561 W, 1557 W and 1459 W. Thus, it is noticed that the JS puzzle pattern of SPTCT configuration has generated relatively higher maximum output power under short narrow condition.

From Table 3, it is observed that the proposed puzzle pattern has an ER ratio of 59.83%, followed by the CSPTCT, OE, KK, LS and SS by 49.33%, 48.83%, 48.80%, 48.67% and 45.58%. Also, the proposed puzzle pattern has a PE ratio of 17.55% in comparison with the conventional configuration, followed by a reduction in performance of the OE, KK, LS and SS by -1.02%, -1.10%, -1.37%, and -8.23% respectively.

4.2.3 BLTCT configuration

Results obtained from the CBLTCT and RBLTCT configurations for the various puzzle pattern with short wide shading condition indicates that the JS puzzle pattern performs superior and generates GMPP of 1982 W (Fig. 16c). The GMPP of the KK is very close to the JS puzzle pattern with GMPP of 1981 W. The OE, SS, LS and CBLTCT follows the performance by 1937 W, 1882 W, 1607 W and 1579 W. Thus, it is noticed that the proposed and KK puzzle pattern of BLTCT configuration has generated almost similar maximum output power under short wide condition.

From Table 3, it is observed that the proposed puzzle pattern has an ER ratio of 61.95%, followed by the KK, OE, SS, LS and CBLTCT configuration by 61.91%, 60.55%, 58.81%, 50.23% and 49.33%. Also, the JS puzzle pattern has a PE ratio of 20.37% in comparison with the CBLTCT, followed by a reduction in performance of the KK, OE, SS, and LS by 20.32%, 18.52%, 16.12%, and 1.80% respectively.

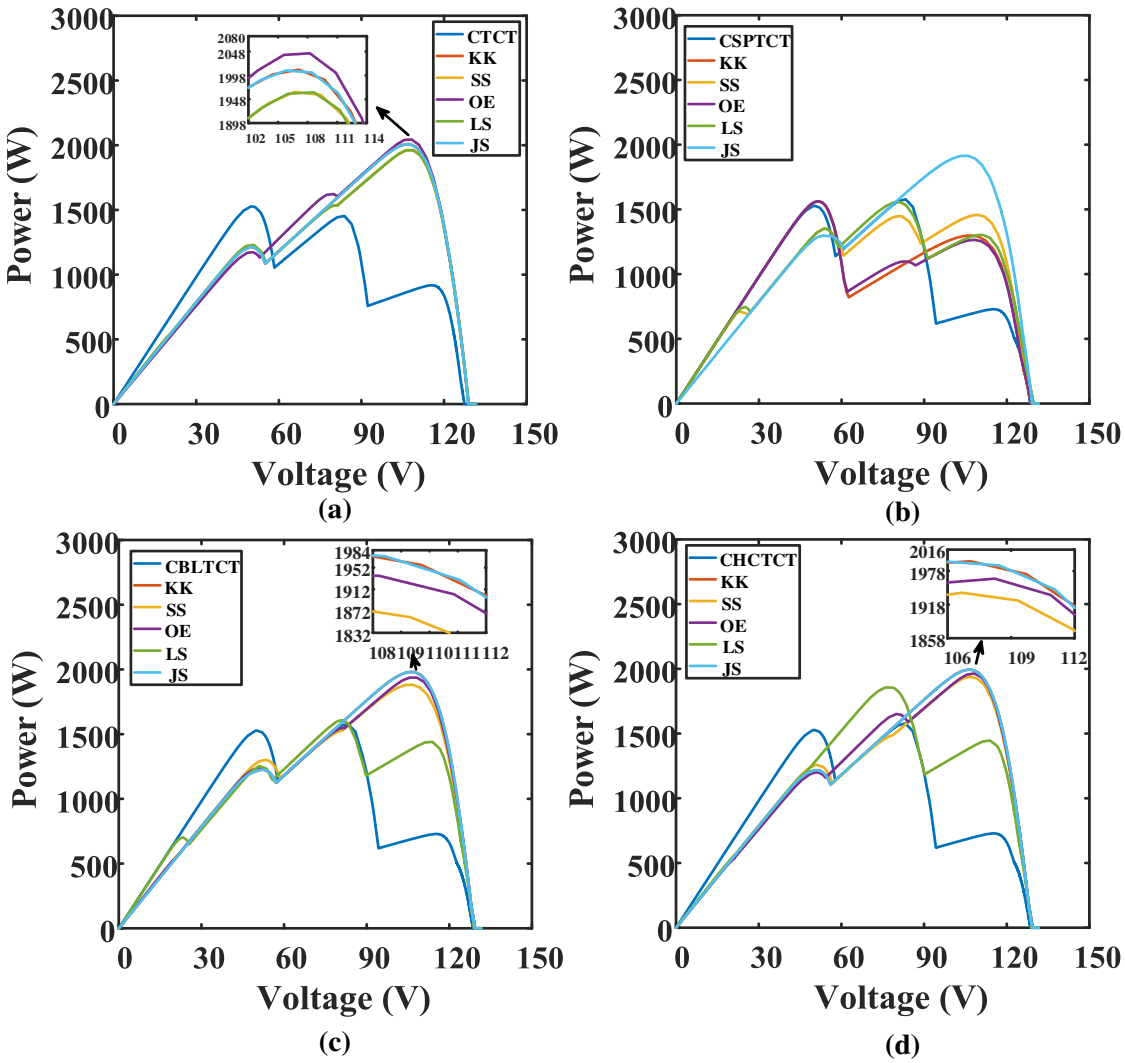

Fig. 16 P-V characteristics: **a** TCT configuration, **b** SPTCT configuration, **c** BLTCT configuration, **d** SPTCT configuration for case 2

4.2.4 HCTCT configuration

Results obtained from the CHCTCT and RHCTCT configurations for the various puzzle pattern with short wide shading condition indicates that the proposed and KK pattern performs superior and generates GMPP of 1995 W (Fig. 16d). The OE, SS, LS and CHCTCT follows the performance by 1964 W, 1939 W, 1857 W and 1579 W. Thus, it is noticed that the proposed and KK puzzle pattern of HCTCT configuration has generated almost similar maximum output power under short wide condition.

From Table 3, it is observed that the JS and KK puzzle pattern has an ER ratio of 62.35%, followed by the OE, SS, LS and CHCTCT by 61.38%, 60.60%, 58.02% and 49.33%. Also, the JS and KK puzzle pattern has a PE ratio of 20.88% in comparison with the CHCTCT, followed by a reduction in performance of the OE, SS, LS by 19.64%, 18.59% and 14.98% respectively.

4.3 Case 3 Long narrow

4.3.1 TCT configuration

Results obtained from the CTCT and RTCT configurations for the various puzzle pattern with long narrow shading condition indicates that the JS puzzle pattern performs superior and generates GMPP of 2148 W (Fig. 17a). The KK, LS, SS, CTCT and OE pattern follows the performance by 2085 W, 1993 W, 1900 W, 1985 W and 1903 W. Thus, it is noticed that the JS puzzle pattern of SPTCT configuration has generated a relatively higher maximum output power under short narrow condition.

From Table 4, it is observed that the JS puzzle pattern has an ER ratio of 67.14%, followed by the KK, LS, SS, CTCT and OE by 65.16%, 62.68%, 62.03%, 59.47% and 59.38%. Also, the JS puzzle pattern has a PE ratio of 11.41% in comparison with the CTCT, followed by a reduction in performance of the KK, LS, SS and OE by 8.73%, 4.51%, 4.12% and reduction in performance by -0.16% respectively.

4.3.2 SPTCT configuration

Results obtained from the CSPTCT and RSPTCT configurations for the various puzzle pattern with long narrow shading condition indicates that the JS puzzle pattern performs superior and generates GMPP of 2000 W (Fig. 17b). The OE, LS, CSPTCT, SS and KK pattern follows the performance by 1924 W, 1896 W, 1865 W, 1844 W and 1832 W. Thus, it is noticed that the JS puzzle pattern of SPTCT configuration has generated a relatively higher maximum output power under long narrow condition.

From Table 4, it is observed that the proposed puzzle pattern has an ER ratio of 62.50%, followed by the OE, LS, CSPTCT, SS and KK pattern by 60.14%, 59.26%, 58.27%, 57.62% and 57.26%. Also, the JS puzzle pattern has a PE ratio of 6.77% in comparison with the CSPTCT, followed by a reduction in performance of the OE, LS, SS and KK pattern by 3.10%, 1.67%, -1.13%, and -1.76% respectively.

Table 4 Simulation results for case 3.

Long Narrow	Puzzle Pattern	V_{mp} (V)	I_{mp} (A)	GMPP (W)	PL (%)	ML (W)	FF (%)	ER (%)	PE (%)
TCT	CTCT	17.56	108.36	1903	40.53	1296.84	44.46	59.47	NA
	KK	19.72	105.77	2085	34.84	1114.72	48.71	65.16	8.73
	SS	18.24	108.81	1985	37.97	1215.00	46.37	62.03	4.12
	OE	24.72	76.88	1900	40.62	1299.92	44.39	59.38	-0.16

Long Narrow	Puzzle Pattern	V_{mp} (V)	I_{mp} (A)	GMPP (W)	PL (%)	ML (W)	FF (%)	ER (%)	PE (%)
	LS	18.39	108.36	1993	37.72	1207.02	46.56	62.28	4.51
	JS	20.28	105.94	2148	32.86	1051.65	50.19	67.14	11.41
SPTCT	CSPTCT	17.21	108.36	1865	41.73	1335.31	43.56	58.27	NA
	KK	17.32	105.77	1832	42.74	1367.60	42.81	57.26	-1.76
	SS	17.37	106.18	1844	42.38	1356.11	43.07	57.62	-1.13
	OE	24.20	79.51	1924	39.86	1275.63	44.95	60.14	3.10
	LS	17.94	105.73	1896	40.74	1303.67	44.30	59.26	1.67
	JS	18.88	105.94	2000	37.50	1199.87	46.72	62.50	6.77
BLTCT	CBLTCT	17.21	108.36	1865	41.73	1335.31	43.56	58.27	NA
	KK	18.96	105.77	2005	37.33	1194.60	46.85	62.67	7.02
	SS	17.99	108.81	1958	38.82	1242.21	45.73	61.18	4.76
	OE	24.62	76.88	1892	40.86	1307.54	44.21	59.14	1.47
	LS	18.05	108.36	1955	38.89	1244.51	45.68	61.11	4.64
	JS	19.69	105.94	2086	34.80	1113.61	48.74	65.20	10.63
HCTCT	CHCTCT	17.31	108.36	1876	41.37	1323.89	43.83	58.63	NA
	KK	19.31	105.77	2042	36.18	1157.63	47.71	63.82	8.14
	SS	18.24	108.81	1985	37.98	1215.47	46.36	62.02	5.46
	OE	24.72	76.88	1900	40.62	1299.92	44.39	59.38	1.26
	LS	18.06	108.36	1957	38.86	1243.49	45.70	61.14	4.11
	JS	19.96	105.94	2114	33.92	1085.57	49.39	66.08	11.27

4.3.3 BLTCT configuration

Results obtained from the CBLTCT and RBLTCT configurations for the various puzzle pattern with long narrow shading condition indicates that the JS puzzle pattern performs superior and generates GMPP of 2086 W (Fig. 17c). The GMPP of the KK is very close to the JS puzzle pattern with GMPP of 2005 W. The SS, LS, OE and CBLTCT pattern follows the performance by 1958 W, 1955 W, 1892 W and 1865 W. Thus, it is noticed that the JS puzzle pattern of BLTCT configuration has generated relatively higher maximum output power under long narrow condition.

From Table 4, it is observed that the JS puzzle pattern has an ER ratio of 62.67%, followed by the KK, SS, LS, OE and CBLTCT by 62.67%, 61.18%, 61.11%, 59.14% and 58.27%. Also, the JS puzzle pattern has a PE ratio of 10.63% in comparison with the CBLTCT, followed by a reduction in performance of the KK, SS, LS, OE pattern by 7.02%, 4.76%, 4.64% and 1.47% respectively.

4.3.4 HCTCT configuration

Results obtained from the CHCTCT and RHCTCT configurations for the various puzzle pattern with long narrow shading condition indicates that the JS puzzle pattern performs superior and generates GMPP of 2114 W (Fig. 17d). The GMPP of the KK is very close to the JS puzzle pattern with GMPP of 2042 W. The SS, LS, OE and CHCTCT follows the performance by 1985 W, 1957 W, 1900 W and 1876 W. Thus, it is noticed that the performance of the JS puzzle pattern generates 72W more output power than the KK pattern. Thus, it is noticed that the JS puzzle pattern of HCTCT configuration has generated relatively higher maximum power output power under long narrow condition.

From Table 4, it is observed that the JS puzzle pattern has an ER ratio of 66.08%, followed by the KK, SS, LS, OE and CHCTCT by 63.82%, 62.02%, 61.14%, 59.38% and 58.63%. Also, the JS puzzle pattern has a PE ratio of 11.27% in comparison with the CHCTCT, followed by a reduction in performance of the KK, SS, LS, OE and CHCTCT by 8.14%, 5.46%, 4.11% and 1.26% respectively.

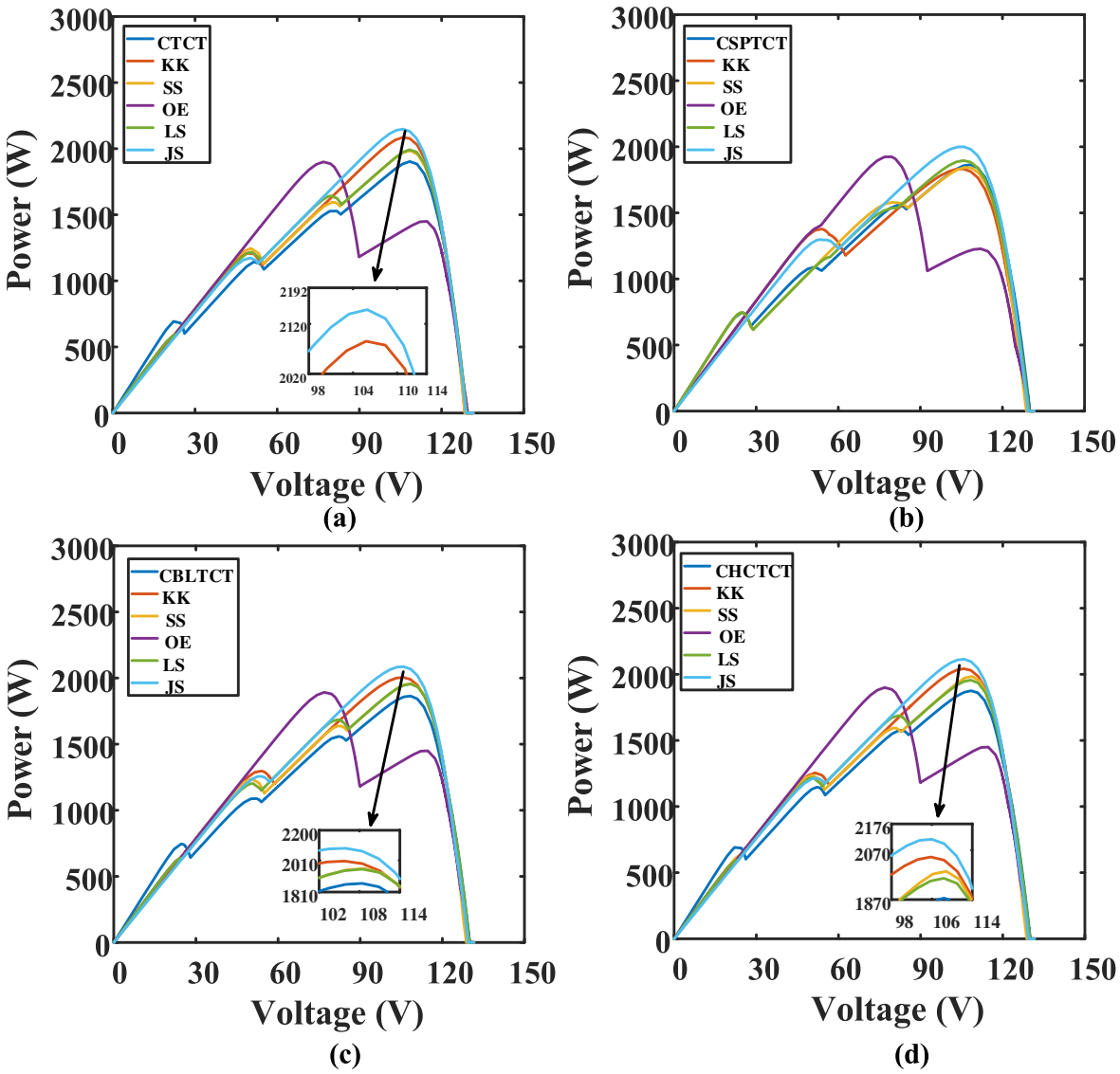

Fig. 17 P-V characteristics: **a** TCT configuration, **b** SPTCT configuration, **c** BLTCT configuration, **d** SPTCT configuration for case 3

4.4 Case 4 Long wide

4.4.1 TCT configuration

Results obtained from the CTCT and RTCT configurations for the various puzzle pattern with long wide shading condition indicates that the KK, SS, LS and JS puzzle pattern performs superior and generates GMPP of 1390 W (Fig. 18a). The CTCT and OE pattern follows the performance by 1306 W and 980 W.

From Table 5, it is observed that the KK, SS, LS and JS puzzle pattern has an ER ratio of 43.43% followed by the CTCT and OE by 40.81%, and 30.64%. Also, the KK, SS, LS and JS puzzle pattern has a PE ratio of 6.03% in comparison with the CTCT, followed by a reduction in performance of the OE pattern by -33.20% respectively.

4.4.2 SPTCT configuration

Results obtained from the CSPTCT and RSPTCT configurations for the various puzzle pattern with long wide shading condition indicates that the LS and the JS puzzle pattern performs superior and generates GMPP of 1349 W (Fig. 18b). The KK, SS, CSPTCT and OE pattern follows the performance by 1339 W, 1339 W, 1305 W and 985 W. Thus, it is noticed that LS and the JS puzzle pattern of SPTCT configuration has generated relatively higher maximum output power under long narrow condition.

From Table 5, it is observed that the LS and the JS puzzle pattern has an ER ratio of 42.17%, followed by the KK, SS, CSPTCT and OE pattern by 41.85%, 41.85%, 40.78% and 30.79%. Also, the LS and the JS puzzle pattern has a PE ratio of 3.28% in comparison with the CSPTCT, followed by the reduction in performance of the KK, SS and OE pattern by 2.54%, 2.54% and -32.45% respectively.

Table 5 Simulation results for case 4.

Long Wide	Puzzle Pattern	V_{mp} (V)	I_{mp} (A)	GMPP (W)	PL (%)	ML (W)	FF (%)	ER (%)	PE (%)
TCT	CTCT	12.46	104.82	1306	59.19	1894.14	30.51	40.81	NA
	KK	13.60	102.19	1390	56.57	1810.35	32.46	43.43	6.03
	SS	13.60	102.19	1390	56.57	1810.35	32.46	43.43	6.03
	OE	19.75	49.65	980	69.36	2219.59	22.90	30.64	-33.20
	LS	13.60	102.19	1390	56.57	1810.35	32.46	43.43	6.03
	JS	13.60	102.19	1390	56.57	1810.35	32.46	43.43	6.03
SPTCT	CSPTCT	12.57	103.81	1305	59.22	1894.92	30.49	40.78	NA
	KK	12.90	103.81	1339	58.15	1860.85	31.28	41.85	2.54
	SS	12.90	103.81	1339	58.15	1860.85	31.28	41.85	2.54
	OE	19.30	51.06	985	69.21	2214.64	23.02	30.79	-32.45
	LS	13.00	103.81	1349	57.83	1850.62	31.52	42.17	3.28
	JS	13.00	13.00	1349	57.83	1850.62	31.52	42.17	3.28
BLTCT	CBLTCT	12.56	103.96	1305	59.21	1894.63	30.49	40.79	NA

Long Wide	Puzzle Pattern	V_{mp} (V)	I_{mp} (A)	GMPP (W)	PL (%)	ML (W)	FF (%)	ER (%)	PE (%)
	KK	13.71	101.33	1389	56.59	1810.76	32.45	43.41	6.04
	SS	13.09	103.96	1361	57.47	1839.08	31.79	42.53	4.08
	OE	19.68	49.82	980	69.36	2219.56	22.90	30.64	-33.14
	LS	13.09	103.96	1361	57.47	1839.01	31.79	42.53	4.09
	JS	13.71	101.33	1389	56.59	1810.76	32.45	43.41	6.04
HCTCT	CHCTCT	12.56	103.95	1305	59.21	1894.64	30.49	40.79	NA
	KK	13.71	101.32	1389	56.59	1810.77	32.45	43.41	6.04
	SS	13.19	103.95	1372	57.14	1828.35	32.04	42.86	4.83
	OE	19.66	49.87	980	69.36	2219.56	22.90	30.64	-33.14
	LS	13.19	103.95	1371	57.14	1828.53	32.04	42.86	4.82
	JS	13.71	101.32	1389	56.59	1810.76	32.45	43.41	6.04

4.4.3 BLTCT configuration

Results obtained from the CBLTCT and RBLTCT configurations for the various puzzle pattern with long wide shading condition indicates that the KK and JS puzzle pattern performs superior and generates GMPP of 1389 W (Fig. 18c). The SS, LS, CBLTCT and OE pattern follows the performance by 1361 W, 1361 W, 1305 W and 980 W. Thus, it is noticed that the KK and JS puzzle pattern of BLTCT configuration has generated relatively higher maximum output power under long narrow condition.

From Table 5, it is observed that the KK and JS puzzle pattern has an ER ratio of 43.41%, followed by the SS, LS, CBLTCT and OE by 42.53%, 42.53%, 40.79% and 30.64%. Also, the KK and JS puzzle pattern have a PE ratio of 6.04% in comparison with the CBLTCT, followed by a reduction in performance of the LS, SS and OE pattern by 4.09%, 4.28% and -33.14% respectively.

4.4.4 HCTCT configuration

Results obtained from the CHCTCT and RHCTCT configurations for the various puzzle pattern with long wide shading condition indicates that the KK and JS puzzle pattern performs superior and generates GMPP of 1389 W (Fig. 18d). The SS, LS, CHCTCT and OE pattern follows the performance by 1372 W, 1371 W, 1305 W and 980 W. Thus, it is noticed that the KK and JS puzzle pattern of HCTCT configuration has generated relatively higher maximum power output power under long narrow condition.

From Table 5, it is observed that the KK and JS puzzle pattern has an ER ratio of 43.41%, followed by the SS, LS, CHCTCT, and OE pattern by 42.86%, 42.86%, 40.79% and 30.64%. Also, the KK and JS puzzle pattern have a PE ratio of 6.04% in comparison with the CHCTCT, followed by a reduction in performance of the SS, LS and OE pattern by 4.83%, 4.82% and -33.14% respectively.

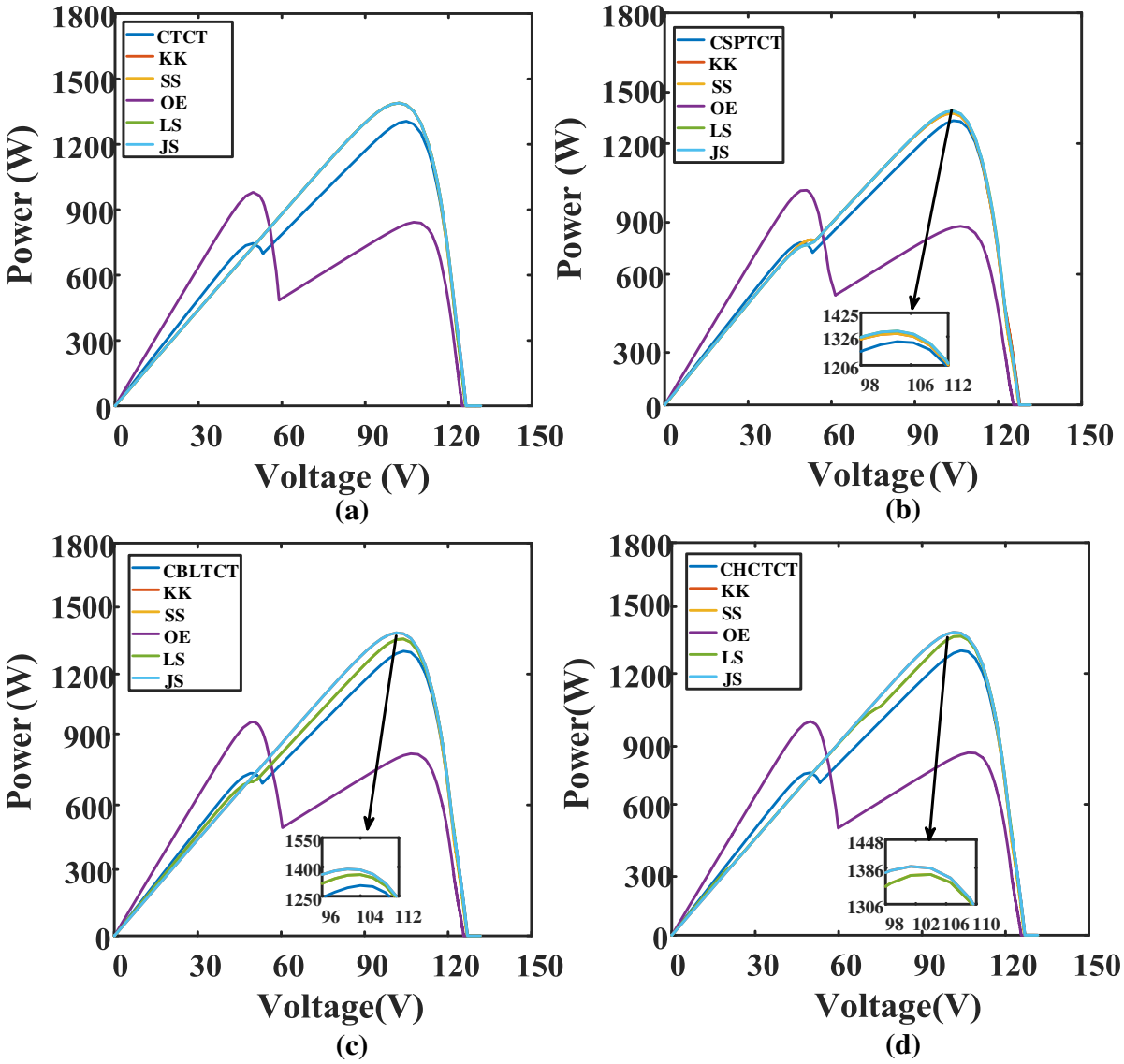

Fig. 18. P-V characteristics: (a) TCT configuration; (b) SPTCT configuration; (c) BLTCT configuration; (d) SPTCT configuration for case 4.

5 Experimental Verification

A detailed experimental setup has been conducted on the 4x4 PV array configuration to validate the effectiveness of the proposed JS puzzle arrangements. The specification of the PV modules considered for the experimental setup is represented in Table 6. Fig. 19 shows the experimental setup of 4×4 PV array configurations. Each module of 10 W is grouped to form a 4×4 PV array configuration. The experimental results for the increasing shading on rows are represented in Table 7.

Table 6 Electrical characteristics of the PV module for experimental verification

Electrical characteristics	Ratings
Maximum Power (P_{max})	10 W
Open circuit voltage (V_{oc})	21.96 V
Voltage at maximum power (V_{mpp})	18.25 V
Short circuit current (I_{sc})	0.59 A
Current at maximum power (I_{mpp})	0.55 A
Number of cells connected in series (N_s)	36

Fig. 19 Experimental setup of 4×4 TCT PV array

In the TCT configuration, KK, SS, LS and JS has produced superior performance followed by the CTCT and OE. In the SPTCT configuration, CSPTCT has produced superior performance followed by the JS, KK, OE, SS and LS. In the BLTCT configuration, SS, LS has produced superior performance followed by the CBLTCT, KK and OE. In the HCTCT configuration SS, LS has produced superior performance followed by the CHCTCT, JS, KK and OE. From the experimental results, it is observed that the TCT configuration has produced superior performance compared to other configuration under the PSCs. The performance of the TCT is followed by the HCTCT, BLTCT and SPTCT configurations

Table 7 Experimental results

Configuration	Puzzle Pattern	(One module shaded) Power (W)	(Two modules shaded) Power (W)	(Three modules shaded) Power (W)	(Four modules shaded) Power (W)
TCT	CTCT	110	110	110	110
	KK	110	117	116	115
	SS	110	117	116	115

Configuration	Puzzle Pattern	(One module shaded) Power (W)	(Two modules shaded) Power (W)	(Three modules shaded) Power (W)	(Four modules shaded) Power (W)
	OE	110	117	79	79
	LS	110	117	116	115
	JS	110	117	116	115
SPTCT	CSPTCT	116	112	115	110
	KK	116	114	84	76
	SS	116	112	84	76
	OE	116	114	84	76
	LS	116	112	84	76
	JS	116	114	84	76
BLTCT	CBLTCT	112	112	110	110
	KK	112	115	81	79
	SS	112	117	115	115
	OE	112	115	81	79
	LS	112	117	115	115
	JS	112	115	81	79
HCTCT	CHCTCT	110	110	110	110
	KK	112	114	115	84
	SS	112	117	116	115
	OE	110	114	81	79
	LS	110	117	115	115
	JS	110	114	115	84

6 Conclusion

In this study, the performance analysis of 4x4 PV array with TCT and hybrid-rearranged configuration is carried out on considered PSCs. The hybrid configuration has fewer numbers ties compared to the conventional configuration to reduce the wiring losses. The mathematical analysis is carried out for a clear understanding of the PV array configurations. Here, the position of the modules in the PV array altered according to the proposed JS puzzle pattern. The investigation is carried out in the MATLAB/SIMULINK environment with a bypass diode connected across each module. The performance of the JS puzzle pattern on hybrid-rearranged configuration is compared to the

existing puzzle patterns in terms of GMPP, PL, ML, FF, ER and PE. Overall, the simulation results obtained by the hybrid-rearranged configuration with JS puzzle based reconfiguration technique has improved the maximum power by 14.01% under the PSCs. The performance of the JS puzzle based reconfiguration technique is followed by the KK, SS, LS and OE puzzle based reconfiguration technique of 10.00%, 5.73%, 5.29% and -3.88% respectively. From the experimental results, it is observed that the KK, SS, LS and JS puzzle pattern based TCT configuration has produced superior results. Overall, the TCT configuration has produced superior performance compared to other configuration under the PSCs. The performance of the TCT is followed by the HCTCT, BLTCT and SPTCT configurations. The results show the effectiveness of the JS puzzle based reconfiguration technique in dispersing the partial shading effects throughout the array compared to existing puzzle based reconfiguration techniques. The JS puzzle based reconfiguration technique reduces the mismatch losses between the rows and mitigates the occurrence of local MPP in the P-V characteristics. In addition, the proposed technique eliminates the need for the complex algorithm, switching matrix and sensors, which is economically viable for the small-scale PV array, whereas the large-scale PV array can be divided into number sub-array. The experimental testing may be conducted to assess the performance of the PV configuration under various shading factors and other experimental factors.

Acknowledgments

The authors thank Dr. Irfan Ahmad Khan, clean and resilient energy systems laboratory, texas a&m university, galveston, usa for the technical expertise provided.

Conflict of Interest Statement

The authors declare no conflict of interest.

References

1. World Energy Council.: World Energy Trilemma Index 2018. Available online: https://www.worldenergy.org/wp-content /uploads/2018/10/World-Energy-Trilemma Index-2018.pdf Accessed on 21 March 2021
2. REN21, Renewables 2019.: Global Status Report 2019. Available online: https://www. ren21.net/wpcontent/uploads/2019/05/gsr_2 019_full_report_en.pdf Accessed on 21 March 2021
3. Palpandian, M., Santhi, M., Padmavathi, M., Sivasankar, V.: An appraisal of rural/urban electricity consumption in a south Indian city: vindication of greener energy potential through solar PV system. Journal of Energy Technology and Policy. **11**(2), 165–182 (2015)
4. Prince Winston D.: Design of Sustainable PV Module for Efficient Power Generation During Faults. IEEE Transactions on components, packaging and manufacturing technology. **10**(3), 389-392 2020
5. Shan Cheng, Tian-Ya Qin, Li-Bing Jing.: Multi-objective optimization of accommodating distributed generation considering power loss, power quality, and system stability. Journal of Industrial and Production Engineering. **31**(3), 146-154 2014
6. Liu, ZF., Li, LL., Tseng, ML., Lim, MK.: Prediction short-term photovoltaic power using improved chicken swarm optimizer - Extreme learning machine model. Journal of Cleaner Production. **248**, 119272 2020
7. Meenakshi Sundaram, B., Manikandan, B.V., Praveen Kumar, B., Prince Winston, D.: Combination of Novel Converter Topology and Improved MPPT Algorithm for Harnessing Maximum Power from Grid

Connected Solar PV Systems. Journal of Electrical Engineering and Technology. **14**(2), 733–746 2019
8. Sakthi Suriya Raj, J.S., Pounraj, P., Prince Winston, D., Ramaraj, R., Cynthia Christabel, S.: Intelligent MPPT Control Technique for Solar PV System. International Journal of Applied Engineering Research. **10**(55), 3386-3391 2015
9. Prince Winston, D., Praveen Kumar, B., Cynthia Christabel, S., Ali, J., Chamkha Ravishankar Sathyamurthy.: Maximum power extraction in solar renewable power system - a bypass diode scanning approach. Computers & Electrical Engineering. **70**, 122-136 2018
10. Bavarinos, K., Dounis, A., Kofinas, P.: Maximum Power Point Tracking Based on Reinforcement Learning Using Evolutionary Optimization Algorithms. Energies. **14**, 335 2021
11. Kampitsis, G., Batzelis, E., Erp, R.V., Matioli, E.: Parallel PV Configuration with Magnetic-Free Switched Capacitor Module-Level Converters for Partial Shading Conditions. Energies. **14**, 456 2021
12. Haq, S., Biswas, S.P., Hosain, M.K., Rahman, M.A,. Islam, M.R,, Jahan, S.: A Modular Multilevel Converter with an Advanced PWM Control Technique for Grid-Tied Photovoltaic System. Energies. **14,** 331 2021
13. Prince Winston, D., Kumaravel, S., Praveen Kumar, B., Devakirubakaran, S.: Performance improvement of solar PV array topologies during various partial shading conditions. Solar Energy. **196**, 228–242 2020
14. Prince Winston, D., Karthikeyan, G., Pravin, M., JebaSingh, O., Akash, A.G., Nithish, S., Kabilan, S.: Parallel power extraction technique for maximizing the output of solar PV array. Solar Energy. **213,** 102–117 2021
15. Prince Winston, D., Karthikeyan, G., Praveen Kumar, B., Devakirubakaran, S., Chitti Babu, B.: Experimental investigation on output power enhancement of partial shaded solar photovoltaic system. Energy Sources Part A: Recovery, Utilization, and Environmental Effects. 2020
16. Pendem Suneel Raju, Suresh Mikkili.: Modelling and performance assessment of PV array topologies under partial shading conditions to mitigate the mismatching power losses. Solar Energy. **160**, 303-321 2018
17. Nnamchi, S.N., Oko, C.O.C., Kamen, F.L., Sanya, O.D.: Mathematical analysis of interconnected photovoltaic arrays under di*ff*erent shading conditions. Cogent Eng. **18** (5), 1507442 2018
18. Mohammadnejad, S., Khalafi, A., Morteza Ahmadi, S.: Mathematical analysis of total-cross-tied photovoltaic array under partial shading condition and its comparison with other configurations. Solar Energy. **133**, 501–511 2016
19. Teo, J.C., Tan, R.H., Ramachandaramurthy, V.K., Tan, C.: Impact of partial shading on the P–V characteristics and the maximum power of a photovoltaic string. Energies. **11**, 1860 2018
20. Belhachat, F., Larbes, C.: Modeling analysis and comparison of solar photovoltaic array configurations under partial shading conditions. Solar Energy. **120**, 399–418 2015
21. Deshkar, S.N., Dhale, S.B., Mukherjee, J.S., Babu, T.S., Rajasekar, N.: Solar PV array reconfiguration under partial shading conditions for maximum power extraction using genetic algorithm. Renewable and Sustainable Energy Review. **43,** 102–110 2015
22. Braun, H., Buddhaa, S.T., Krishnan, V.: Topology reconfiguration for optimization of photovoltaic array output. Sustain Energy Grids Networks. **6**, 58-69 2016
23. Babu, T.S., Ram, J.P., Dragičević, T., Miyatake, M., Blaabjerg, F., Rajasekar, N.:

Particle swarm optimization based solar PV array reconfiguration of the maximum power extraction under partial shading conditions. IEEE Trans. Sustain. Energy. **9**(1), 74–85 2018

24. InduRani, B., Ilango, G., Saravana Nagamani, Chilakapati.: Enhanced Power Generation From PV Array Under Partial Shading Conditions by Shade Dispersion Using Su Do Ku Configuration. IEEE Transaction on Sustainable Energy. **4**(3), 594–601 2013
25. Vijayalekshmy, V., Bindu, G.R., Iyer, SR.: Performance improvement of partially shaded photovoltaic arrays under moving shadow conditions through shade dispersion. J. Inst. Eng. (India) Ser. **0,** 1–7 2015
26. Srinivasa Rao Potnuru, Dinesh Pattabiraman, Saravana Ilango Ganesan, Nagamani Chilakapati.: Positioning of PV panels for reduction in line losses and mismatch losses in PV array. Renewable Energy. **78**, 264–275 2015
27. Yadav Anurag Singh, Pachauri Rupendra Kumar, Chauhan, Yogesh, K., Choudhury, S., Singh Rajesh.: Performance enhancement of partially shaded PV array using novel shade dispersion effect on magic-square puzzle configuration. Solar Energy. **144**, 780–797 2017
28. Vijayalekshmy, S., Bindu, G.R., Rama Iyer, S.: A novel Zig-Zag scheme for power enhancement of partially shaded solar arrays. Solar Energy. **135**, 92–102 2016
29. Manoharan Premkumar, Umashankar Subramaniam, Thanikanti Sudhakar Babu, Rajvikram Madurai Elavarasan, Lucian Mihet-Popa.: Evaluation of Mathematical Model to Characterize the Performance of Conventional and Hybrid PV Array Topologies under Static and Dynamic Shading Patterns. Energies. **13**, 3216 2020
30. Dhanup, S.P, Rajasekar, N., Ram, J.P., Chinnaiyan, V.K.: Design and testing of two phase array reconfiguration procedure for maximizing power in solar PV systems under partial shade conditions (PSC). Energy Conversation and Management. **178**, 92–110 2018
31. Renaudineau, H., Houari, A., Martin, J.P., Pierfederici, S., Meibody, T.F., Gerardin, B.: A new approach in tracking maximum power under partially shaded conditions with consideration of converter losses. Solar Energy **85**, 2580–2588 2011
32. Yadav, A.S., Pachauri, R.K., Chauhan, Y.K.: Comprehensive Investigation of PV arrays with puzzle shade dispersion for improved performance. Solar Energy. **129**, 256–285 2016
33. Pachauri, R.K., Yadav, A.S., Chauhan, Y.K., Sharma, A., Kumar, V.: Shade dispersion-based photovoltaic array configurations for performance enhancement under partial shading conditions. Int. Trans. Electr. Energy Syst. **28**, 2556–2587 2018
34. Sai Krishna, G., Tukaram Moger.: Enhancement of maximum power output through reconfiguration techniques under non-uniform irradiance conditions. Energy. **187**, 115917 2019
35. Ibraheem Nasiruddin, Shahida Khatoon, Mohd Faisal Jalil, Bansal RC. Shade diffusion of partial shaded PV array by using odd-even structure. Solar Energy. **181**, 519–529 2019
36. Rupendra Pachauri, Anurag Singh Yadav, Yogesh, K., Chauhan, Abhinav Sharma, Vinod Kumar.: Shade dispersion-based photovoltaic array configurations for performance enhancement under partial shading conditions. Int Trans Electr Energ Syst. 2556 2018
37. Villalva, M.G., Gazoli, J.R., Filho, E.R.: Comprehensive Approach to Modeling and Simulation of Photovoltaic Arrays. IEEE Transactions on Power Electronics. **24**(5), 1198-1208 2009

38. Vengatesh, R.P., Edward Rajan, S.E.: Analysis of PV module connected in different configurations under uniform and non-uniform solar radiations. International Journal of Green Energy. **13**(14), 1507–1516 2016
39. Dhimish, M., Holmes, V., Mehrdadi, B., Dales, M., Chong, B., Zhang, L.: Seven indicators variations for multiple PV array configurations under partial shading and faulty PV conditions. Renewable Energy. **113**, 438-460 2017
40. Nayak, B., Mohapatra, A., Das, P.: Optimal hybrid array configuration scheme to reduce mismatch losses of photovoltaic system. In Proceedings of the Second International Conference on Electrical, Computer and Communication Technologies (ICECCT). 1-7 2017

Figures

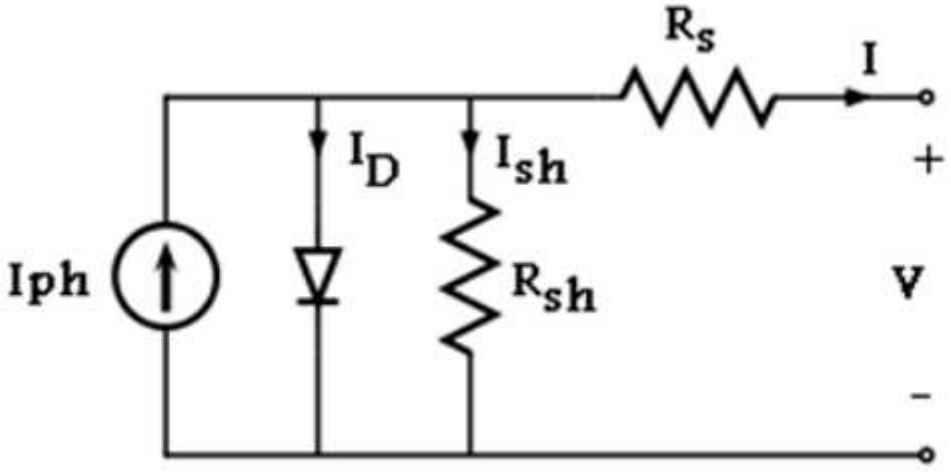

Figure 1

Please see the Manuscript PDF file for the complete figure caption

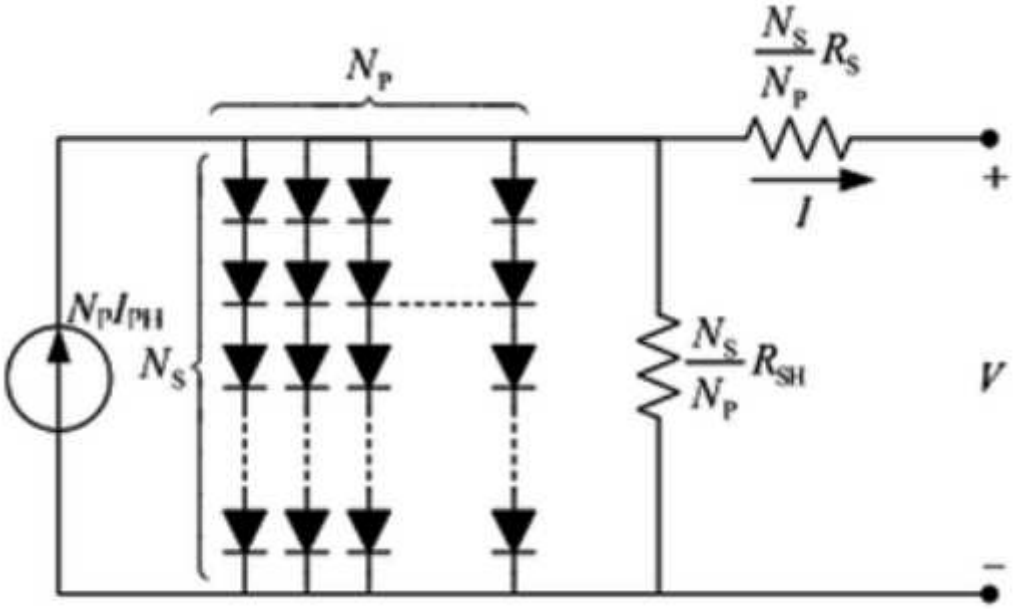

Figure 2

Please see the Manuscript PDF file for the complete figure caption

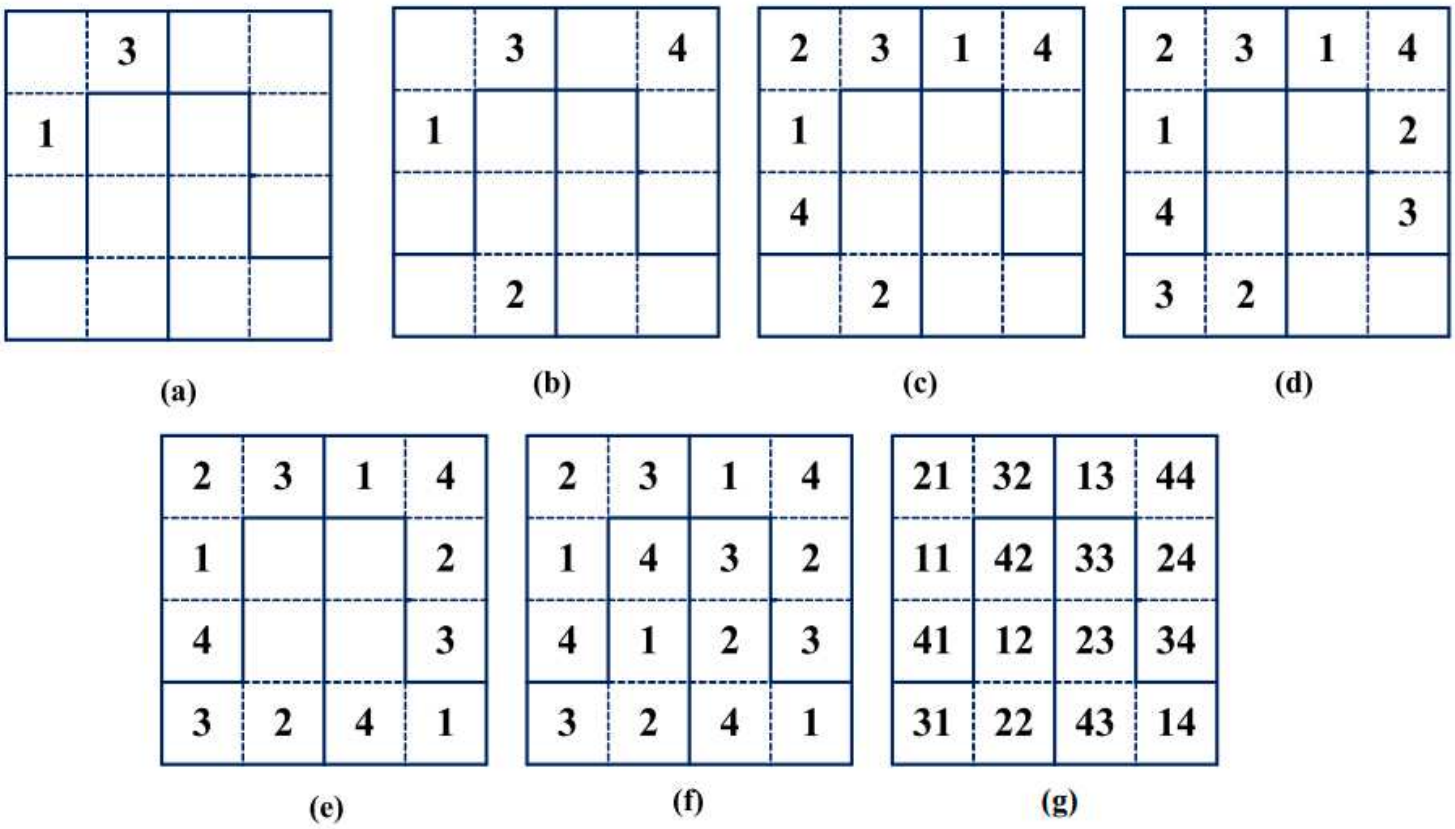

Figure 3

Please see the Manuscript PDF file for the complete figure caption

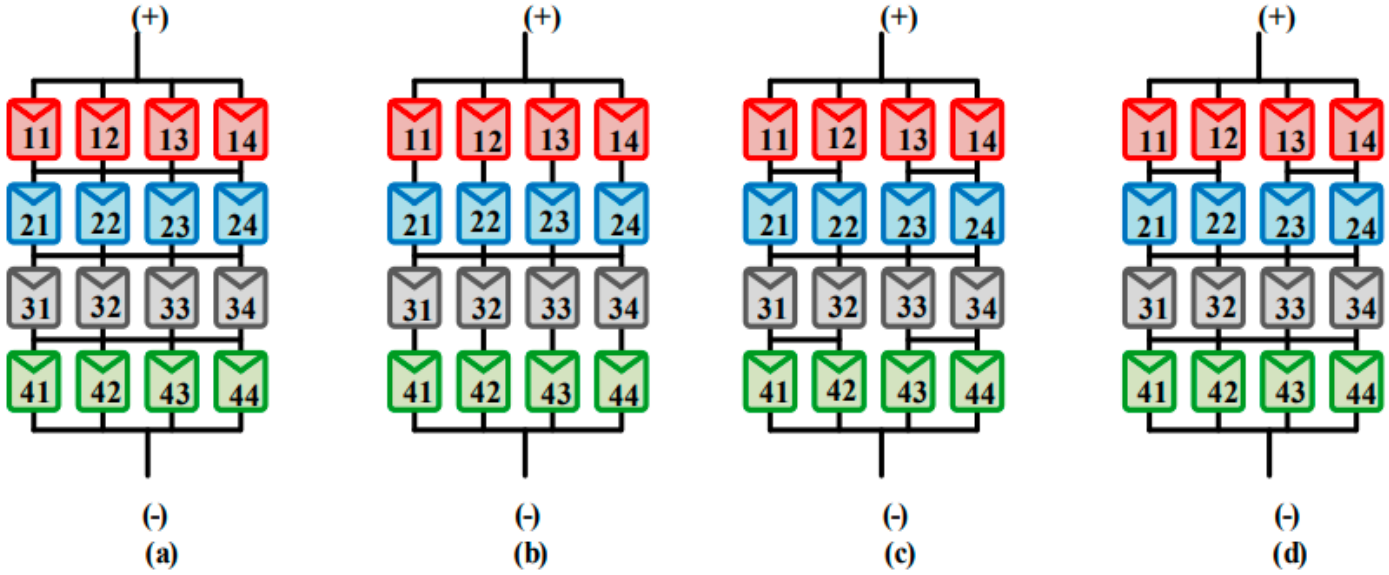

Figure 4

Please see the Manuscript PDF file for the complete figure caption

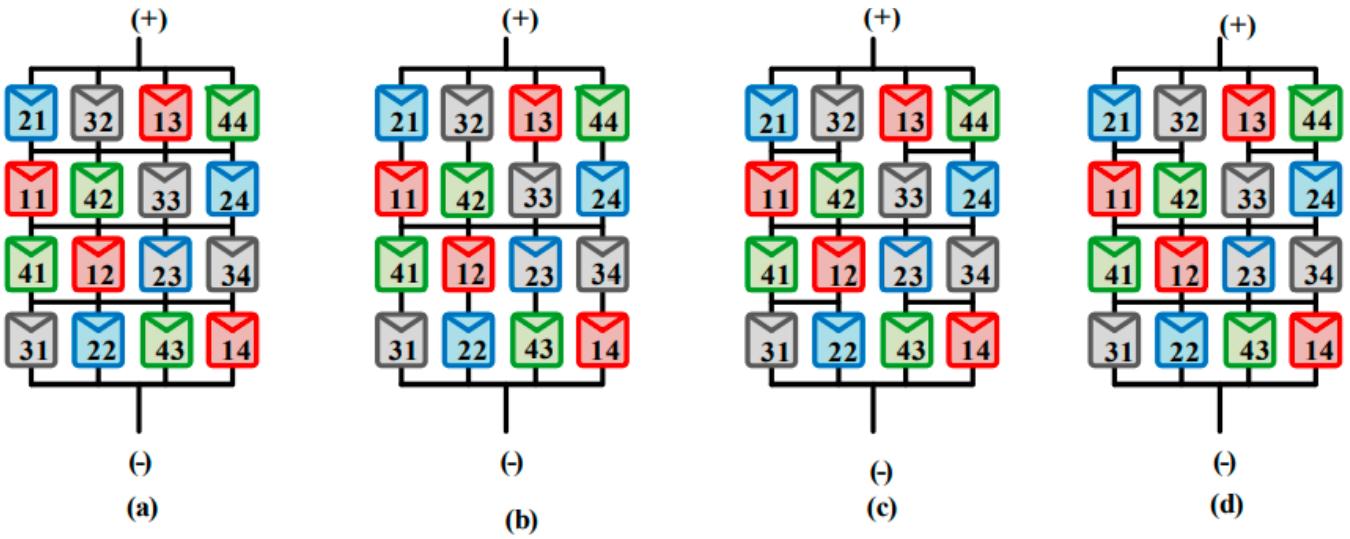

Figure 5

Please see the Manuscript PDF file for the complete figure caption

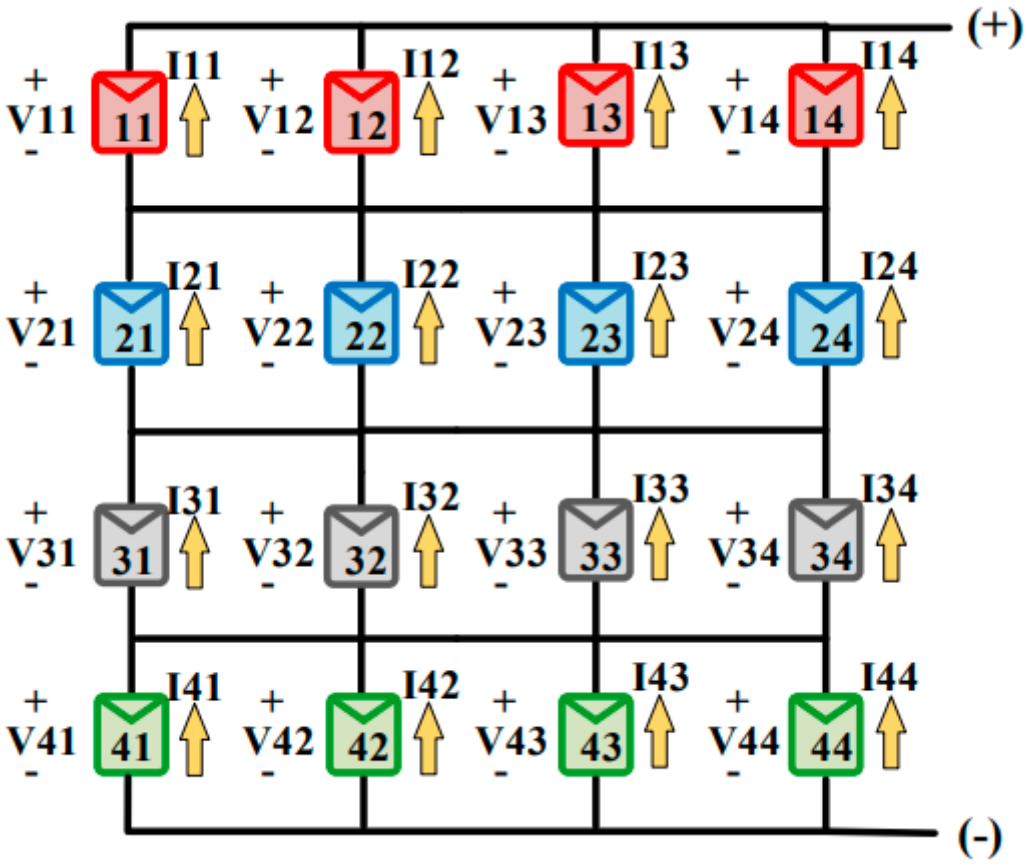

Figure 6

Please see the Manuscript PDF file for the complete figure caption

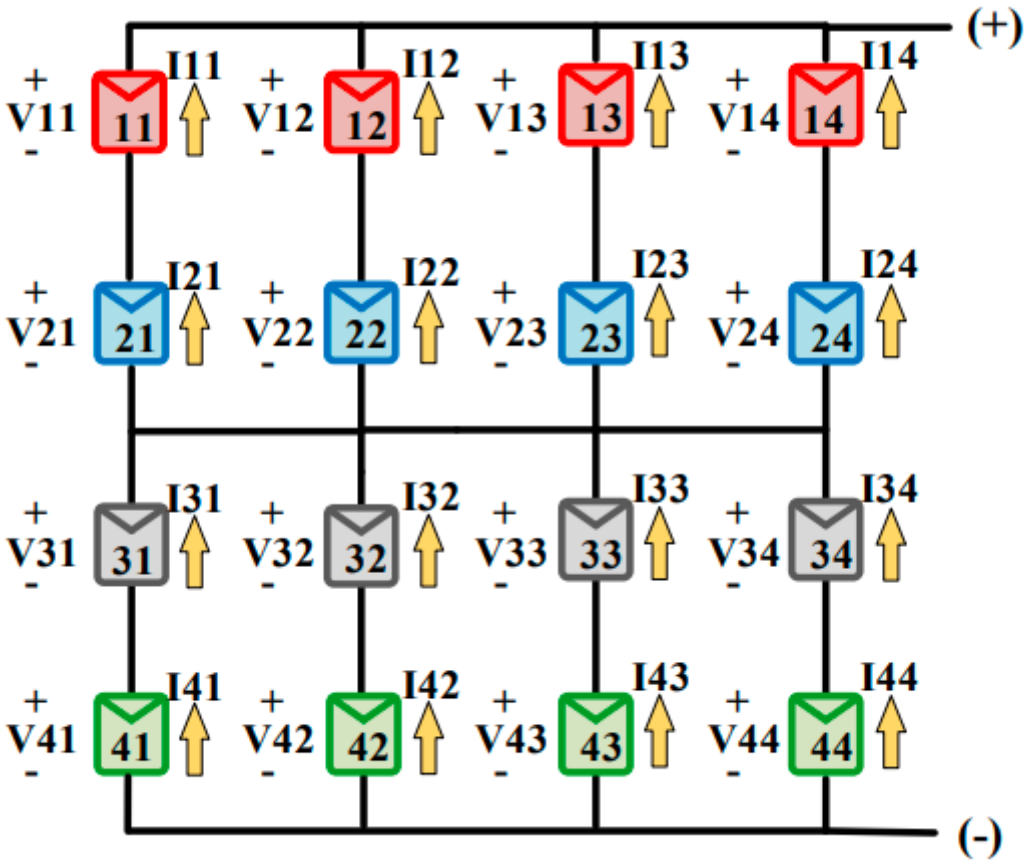

Figure 7

Please see the Manuscript PDF file for the complete figure caption

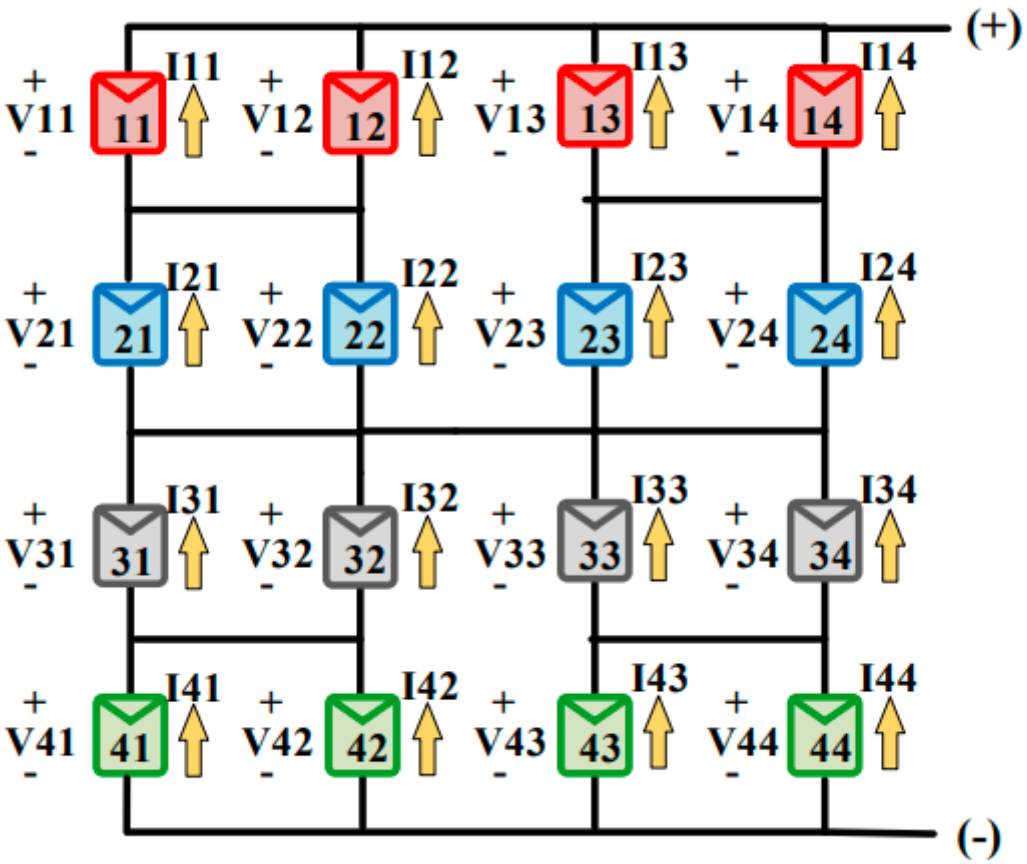

Figure 8

Please see the Manuscript PDF file for the complete figure caption

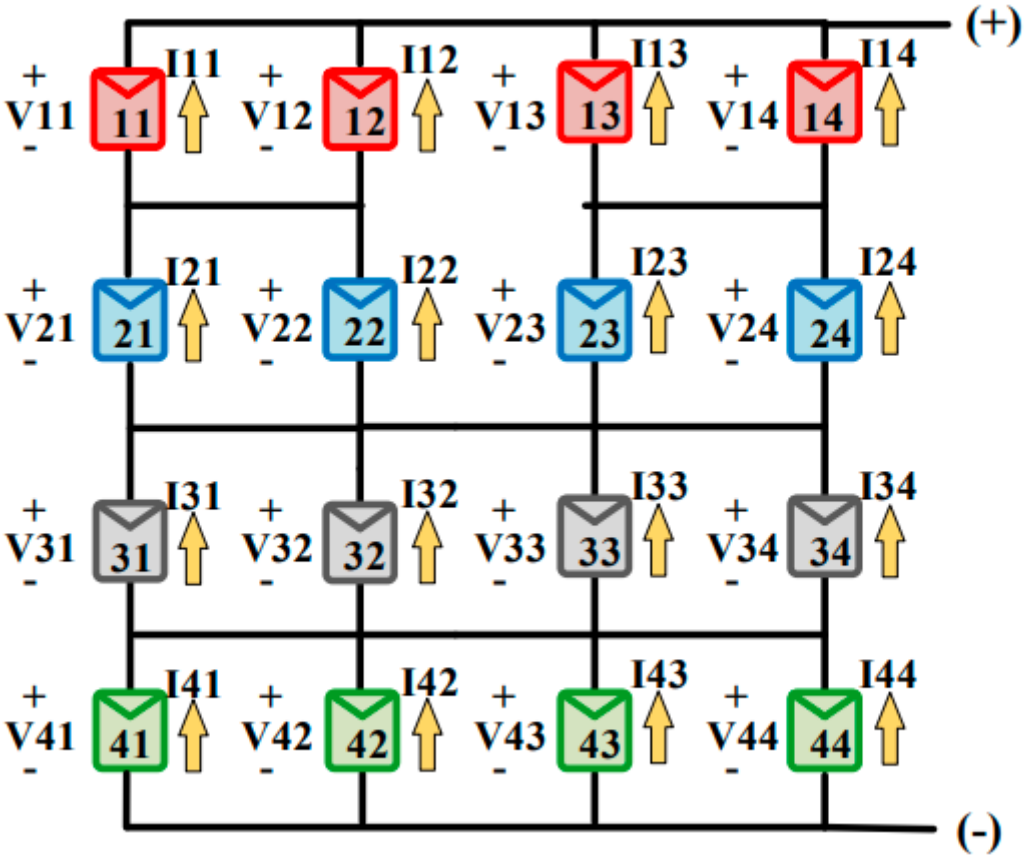

Figure 9

Please see the Manuscript PDF file for the complete figure caption

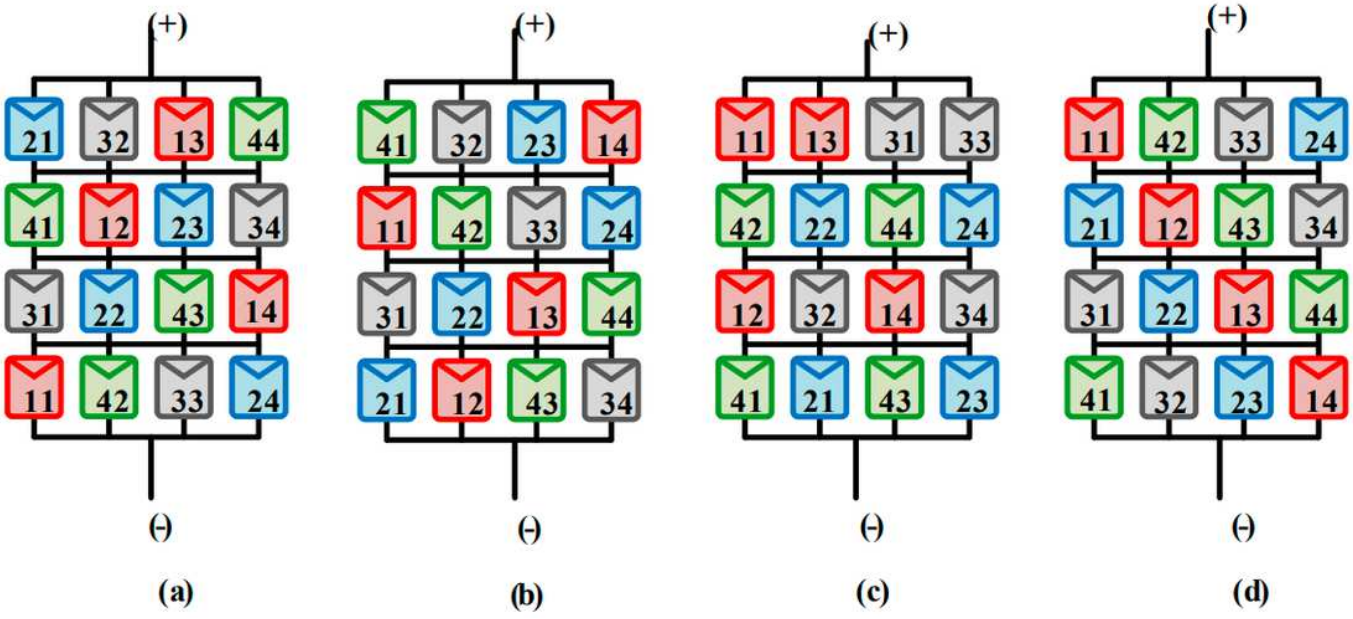

Figure 10

Please see the Manuscript PDF file for the complete figure caption

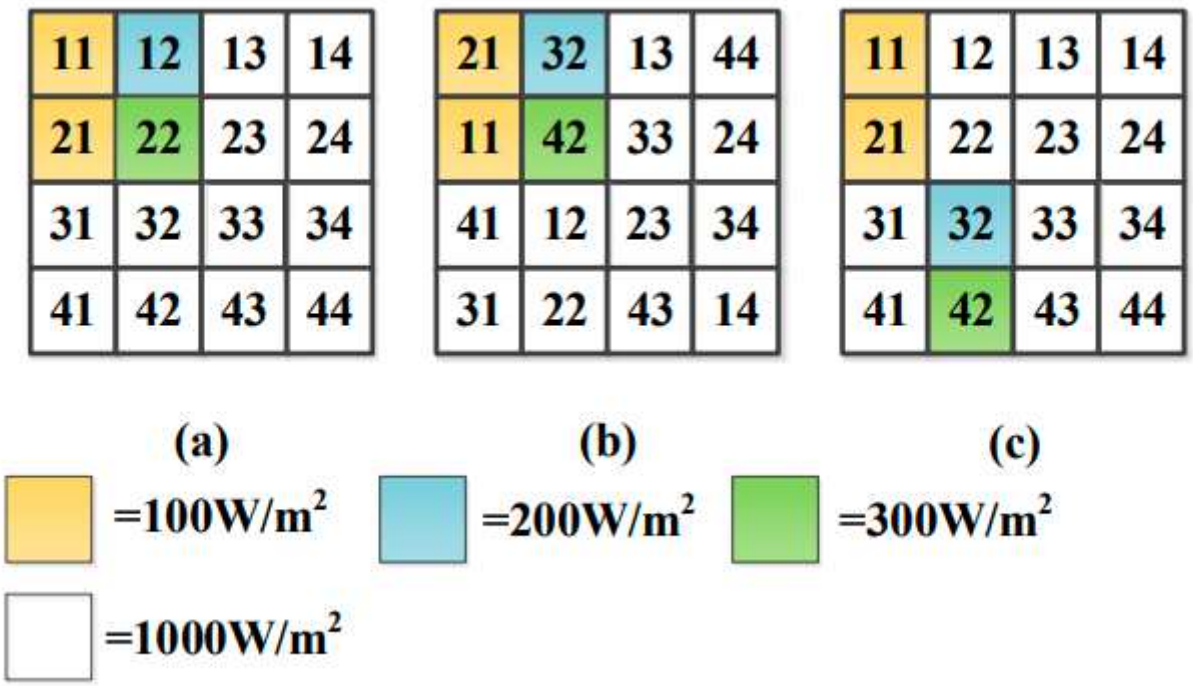

Figure 11

Please see the Manuscript PDF file for the complete figure caption

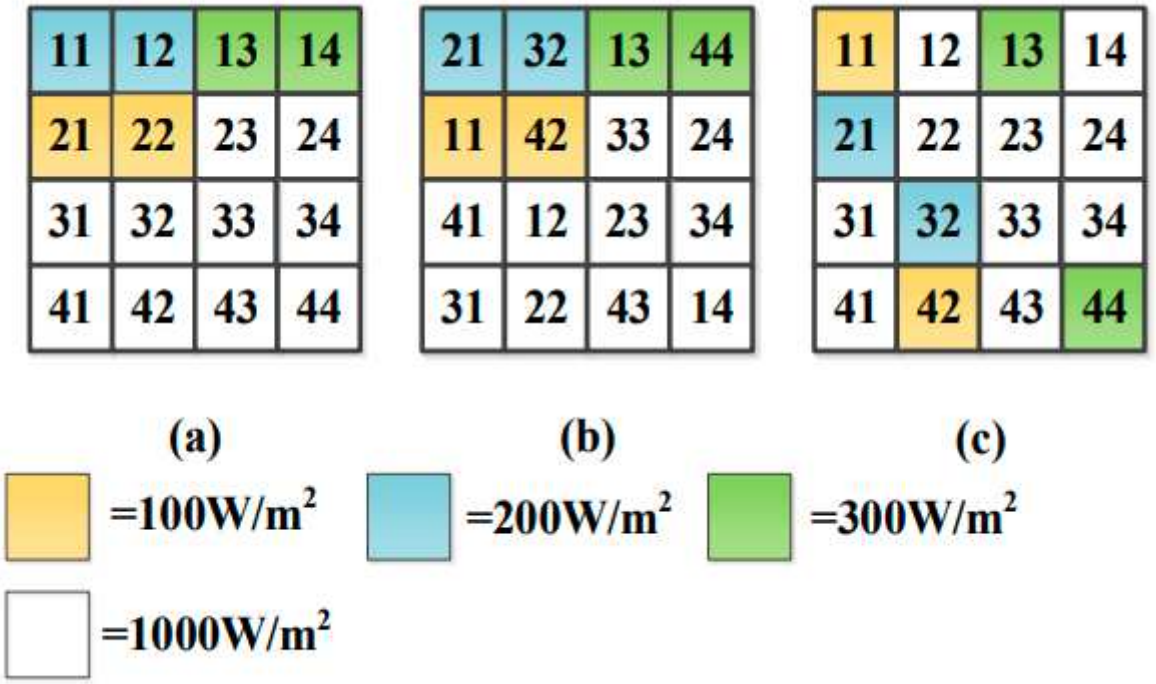

Figure 12

Please see the Manuscript PDF file for the complete figure caption

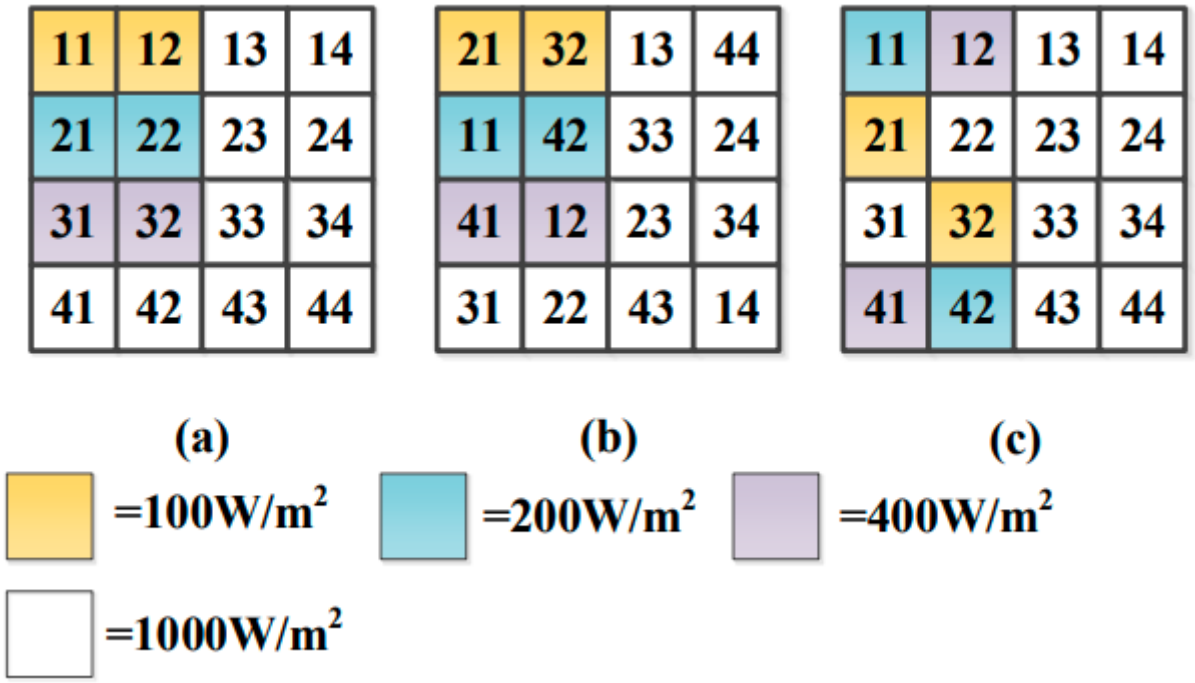

Figure 13

Please see the Manuscript PDF file for the complete figure caption

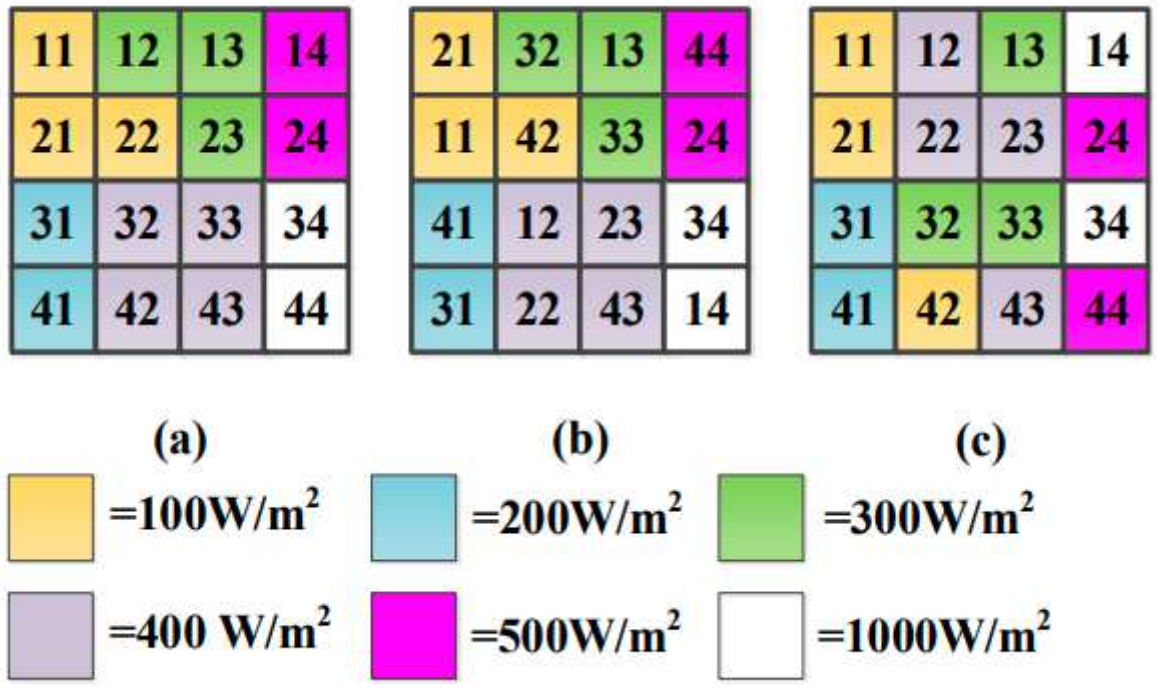

Figure 14

Please see the Manuscript PDF file for the complete figure caption

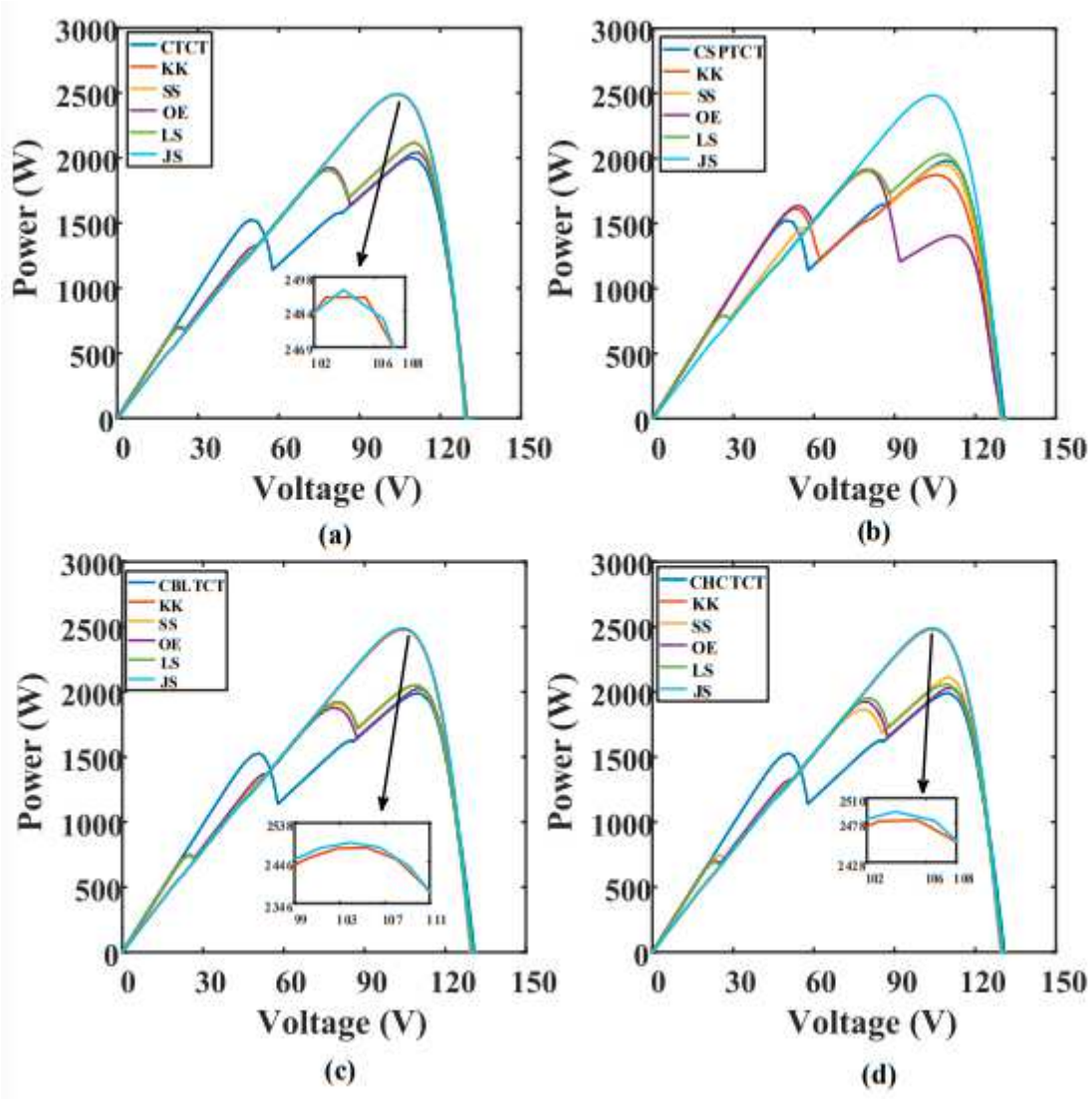

Figure 15

Please see the Manuscript PDF file for the complete figure caption

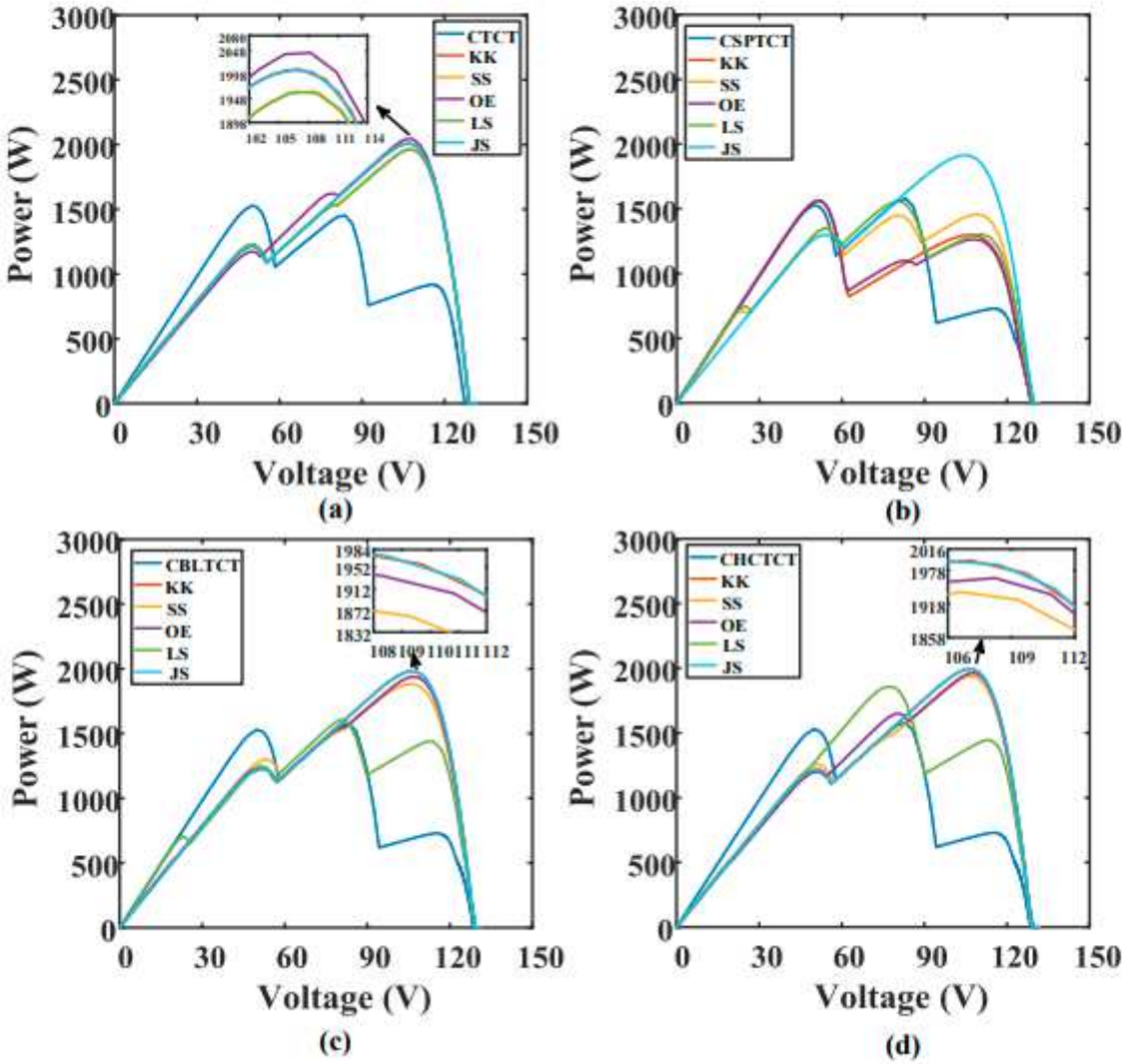

Figure 16

Please see the Manuscript PDF file for the complete figure caption

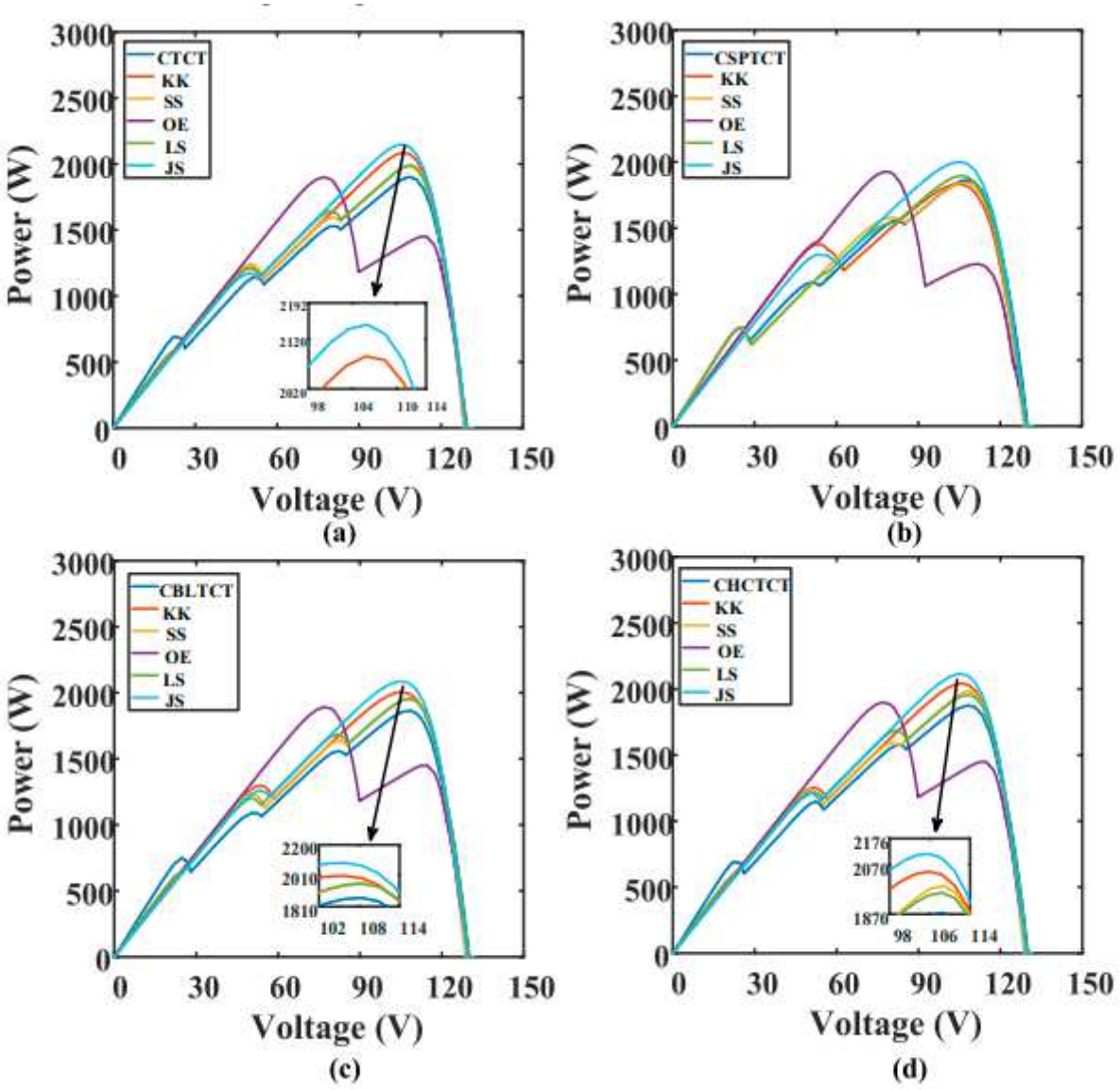

Figure 17

Please see the Manuscript PDF file for the complete figure caption

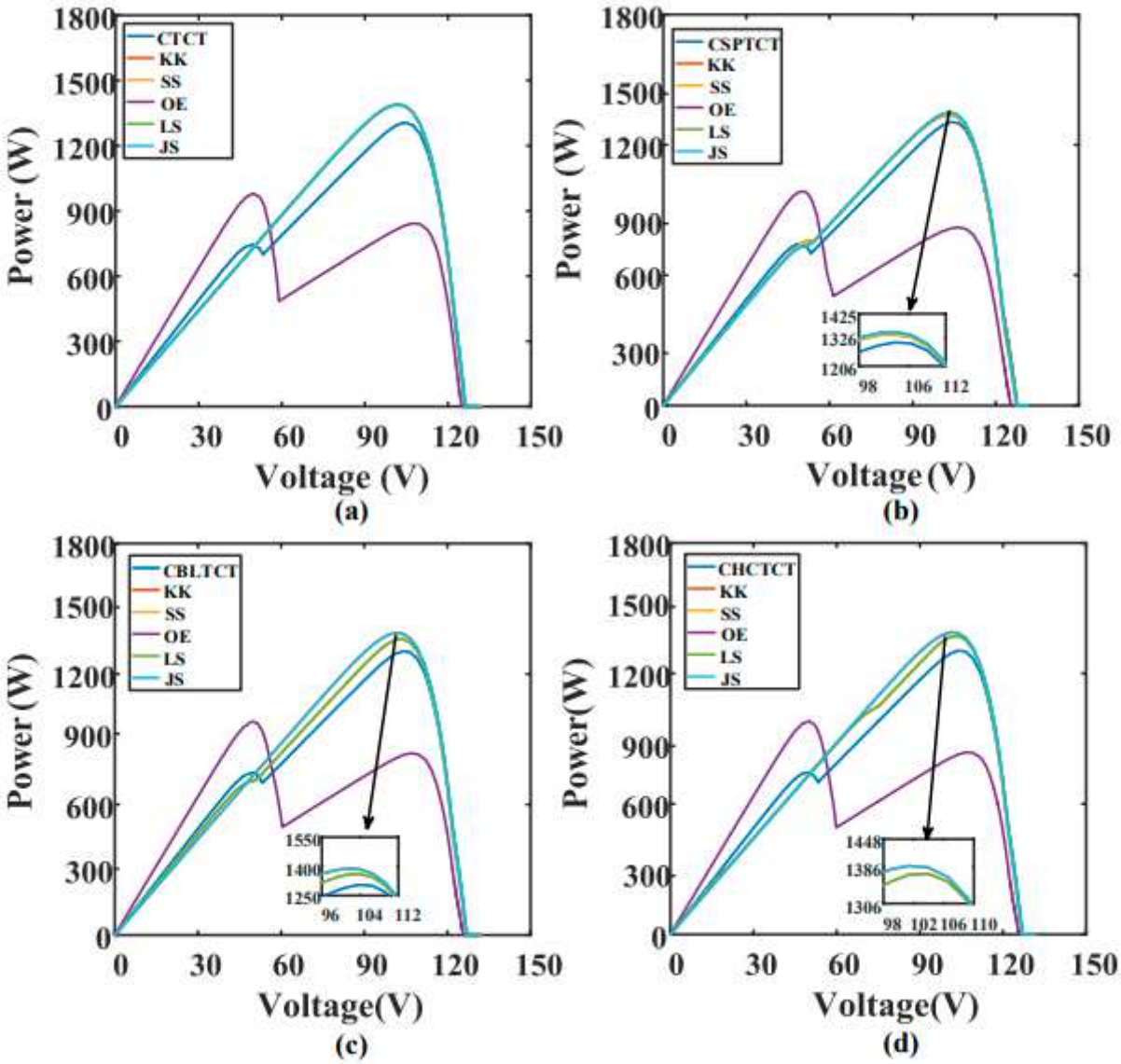

Figure 18

Please see the Manuscript PDF file for the complete figure caption

Figure 19

Please see the Manuscript PDF file for the complete figure caption